NASA Technical Paper 1320

Aerothermal Tests of a Heat-Pipe-Cooled Leading Edge at Mach 7

Charles J. Camarda

NOVEMBER 1978

NASA

NASA Technical Paper 1320

Aerothermal Tests of a Heat-Pipe-Cooled Leading Edge at Mach 7

Charles J. Camarda
Langley Research Center
Hampton, Virginia

National Aeronautics
and Space Administration

**Scientific and Technical
Information Office**

1978

SUMMARY

A sodium-filled, Hastelloy[1] X, heat-pipe-cooled leading-edge model, which had previously been tested in a radiant-heating environment, was subjected to steady-state, Earth-entry aerothermal loads (heat and pressure) in the Langley 8-foot high-temperature structures tunnel to verify performance in a realistic hypersonic environment. The model was tested at angles of attack of 0°, 10°, and 20°, angles of roll of 0° and 90°, calculated stagnation heating rates ranging from 244 to 422 kW/m^2 (21.5 to 37.2 Btu/ft^2-s), and nominal stagnation pressures of about 50 and 124 kPa (7.3 and 18 psia). The heat pipes operated isothermally for these test conditions with maximum operating temperatures ranging from 950 to 1100 K (1250° to 1520° F).

Near steady-state temperatures obtained during the aerothermal tests were in good agreement with analytical results. Pressure and calculated heat-flux distributions were also in good agreement with design distributions. The results indicate that heat pipes can accommodate very intense localized heating and effectively isothermalize structural components. Specifically, results of the tests indicate that the use of heat pipes for leading-edge cooling is a feasible method for lowering localized stagnation temperatures of hypersonic cruise vehicles and space transportation system vehicles sufficiently to allow the use of available and durable superalloys for such applications.

INTRODUCTION

The wing leading edge is a critical area of reusable space transportation system vehicles because of the hostile thermal environment experienced during Earth entry. Temperatures along the stagnation line of an uncooled leading edge can exceed the thermal-structural capabilities of metals; hence the use of carbon-carbon, ceramic, or ablative materials is necessary. Also, large temperature gradients produced by variations in aerodynamic heating near the stagnation line can induce thermal stresses in uncooled leading edges (ref. 1) unless complex load-alleviating features are incorporated in the structural design.

Heat pipes have been examined analytically as a means of lowering peak temperatures and alleviating thermal gradients associated with leading edges of reusable entry vehicles (refs. 1 to 4). A comparison of a heat-pipe-cooled concept with ablative, carbon-carbon, and coated-columbium leading edges in references 2 and 3 suggests the viability of the heat-pipe-cooled concept. Radiant-heat tests of a Hastelloy X, heat-pipe-cooled leading edge (ref. 5) demonstrated successful startup, transient, and steady-state thermal performance at design heating levels.

---

[1]Hastelloy: Trademark of Union Carbide Corp.

The purpose of the present study is to verify performance of the leading edge in a realistic hypersonic aerothermal environment. A total of 8 aerothermal tests in the Langley 8-foot high-temperature structures tunnel and 25 supplemental radiant-heat cycles were completed during the study. Model behavior at various angles of roll (0° and 90°), angles of attack (0°, 10°, and 20°), and heat load levels was studied to determine the effect of these parameters on heat-pipe performance. Maximum hot-wall stagnation heating rates ranged from 244 to 422 kW/m^2 (21.5 to 37.2 Btu/ft^2-s) with maximum operating temperatures ranging from 950 to 1100 K (1250° to 1520° F) for an average aerothermal test time of 30 seconds. Results of the aerothermal tests are presented and compared with design conditions.

Use of trade names or names of manufacturers in this report does not constitute an official endorsement of such products or manufacturers, either expressed or implied, by the National Aeronautics and Space Administration.

SYMBOLS

Values are given in both SI Units and U.S. Customary Units. Measurements and calculations were made in U.S. Customary Units.

l	chordwise surface distance measured from nose, m (ft)
l_T	total chordwise surface distance from nose to end of leading edge, m (ft)
M	Mach number
p	pressure, Pa (psia)
q	dynamic pressure, Pa (lbf/ft^2)
$\dot{q}$	heat input, W/m^2 (Btu/ft^2-s)
R	unit Reynolds number, per m (per ft)
T	temperature, K ($^{\circ}F$ or $^{\circ}R$)
w	one-half total width of wind-tunnel model, m (ft)
x	coordinate measured from center of model along span (see table I), m (ft)
α	angle of attack, deg
ΔT	difference in temperature, K ($^{\circ}F$)
ϕ	angle of roll, deg

Subscripts:

c	combustor
s	model stagnation conditions
t	total conditions
∞	free stream

MODEL, APPARATUS, AND TESTS

Model

The test model (see fig. 1) is approximately a one-half-scale thermal model of a heat-pipe-cooled leading edge that was designed for a Phase B shuttle orbiter configuration (refs. 3 and 4). It was previously tested in a radiant heating environment (ref. 5) only. The model has a span of 15 cm (6 in.) and a chord length of 56 cm (22 in.). It consists of 12 sodium-charged, Hastelloy X, heat pipes brazed to the inner surface of a thin (0.05-cm (0.02-in.)) Hastelloy X aerodynamic skin. Sodium was chosen as the working fluid because of its high heat transport capacity and its compatibility with nickel-base superalloys at expected operating temperatures. The heat pipes have an outer diameter of 1.27 cm (0.5 in.), a wall thickness of 0.127 cm (0.05 in.), and a wick thickness of 0.089 cm (0.035 in.). The wick is a concentric annulus design consisting of seven alternate layers of 100- and 200-mesh stainless steel screen. The 200-mesh screen is located at the outer and inner surfaces of the wick to insure good liquid contact to the tube wall and a high capillary pumping capability. The cross-sectional area of the test-model wick was scaled, as described in reference 4, to equilibrate the capillary pumping head for both the flight test and a 10° angle-of-attack test. Satisfactory performance of the test model when pitched 10° upward from the horizontal for typical reentry heat loads would, therefore, insure adequate wick capability of the flight design. The aerodynamic surface of the leading edge was coated with a high-emissivity ceramic paint to facilitate heat rejection by radiation. The application and operation of heat pipes for leading-edge cooling are explained in reference 5.

Oil-flow studies (discussed in the appendix) indicated that two (stainless steel) span extensions and aerodynamic fences, attached to either side of the heat-pipe model as shown in figure 2, would be necessary to insure two-dimensional flow over the heat-pipe model. The aerodynamic fences, which extend several centimeters above the surface of the leading edge, were beveled to produce a minimal effect on flow over the surface of the test model. The extensions were water-cooled and the outer surfaces of the extensions were flame sprayed with zirconium coating for thermal protection. To prevent heat loss to the inner cavity of the model, the surface of the heat pipes inside

the model was covered with Fiberfrax[2] insulation (2.5 cm (1 in.) thick) and a thin sheet of stainless steel (0.013 cm (0.005 in.) thick). The inner cavity was purged with gaseous nitrogen during the aerothermal tests to prevent hot gas ingress.

Instrumentation

Thirty-five chromel-alumel thermocouples were spotwelded to the outer surface of the heat pipes inside the model (fig. 1) and located as listed in table I. Twenty-seven surface pressure orifices were installed in the extension sections as shown in figure 3 and at locations listed in table II. Pressures were measured with strain-gage-type pressure transducers, connected to the 0.15-cm (0.06-in.) inner-diameter orifice by tubing approximately 91 cm (36 in.) in length. Thin-foil heat-flux gages were mounted on the aerodynamic surface of the extensions (fig. 2), but erosion damage rendered them inoperable early in the test series.

Data Acquisition and Reduction

Outputs of the thermocouples and pressure transducers were recorded at a rate of 20 frames per second by a steady-state recording system. The experimental and analytical quantities reported herein are based on the thermal, transport, and flow properties of the combustion-products test medium as determined from reference 6. Free-stream test-section conditions are related to combustor conditions and were determined from tunnel survey tests.

Facility

The tests were performed in the Langley 8-foot high-temperature structures tunnel (8-ft HTST), which is a hypersonic blowdown tunnel in which the high-energy level for simulating hypersonic flight is attained by burning methane and air in a high-pressure combustor. The resulting combustion gases are expanded through an axisymmetric-contoured 2.44-m (8-ft) exit-diameter nozzle to obtain a nominal Mach 7 flow in an enclosed 4.27-m (14-ft) long open-jet test section. The facility is capable of simulating nominal Mach 7 flight conditions for altitudes from 24 400 to 39 600 m (80 000 to 130 000 ft) for test times up to 200 seconds, depending upon the combustor pressure. Previous studies (refs. 6 and 7 to 9) in the 8-foot HTST indicated that the aerodynamic heating and loading coefficients obtained in the combustion-products test medium of this facility are comparable with those obtained in air facilities. Additional details of the facility can be found in reference 10.

The test model was cantilevered from a curved water-cooled strut and mounted on a hydraulically operated elevator which can insert the model into the stream or retract the model from the stream in approximately 1 second. Before and after each test the model is retracted and covered in the pod below the test section by a pair of acoustic baffles which protect the model from

---

[2]Fiberfrax: Trademark of Harbison-Carborundium Corp.

potentially damaging acoustic disturbance and buffeting generated during facility startup and shutdown. Radiant heaters, similar to those used in reference 5, are available to preheat the test model and are located below the baffles. The model (in the 90° roll position) and heater arrays are shown in figure 4. The heaters, which surround the model, were used in opposing arrays to heat the aerodynamic surface of the heat-pipe model.

Test and Test Procedure

The model test conditions are listed in table III. Nominal tunnel test conditions were: $T_{t,c} \cong 1962$ K (3500° R); $M_\infty \cong 7$; $q_\infty \cong 25$ and 67 kPa (520 and 1400 lbf/ft^2); $R_\infty \cong 1.7 \times 10^6$ and 4.4×10^6 per m (0.52×10^6 and 1.3×10^6 per ft); $\alpha = 0°$, 10°, and 20°; $\phi = 0°$ and 90°; and an angle of yaw of 0°. These conditions correspond to model stagnation pressures of about 50 and 124 kPa (7.3 and 18 psia); precise test values are listed in table III. The model was subjected to eight aerothermal tests which lasted approximately 30 seconds each during which maximum heat-pipe operating temperatures ranged from 950 to 1100 K (1250° to 1520° F).

The short run time in the wind tunnel and high heat pulse of the 8-foot HTST necessitated preheating the model to assure heat-pipe startup. Consequently only steady-state aerothermal performance was investigated. The model was subjected to 25 supplemental radiant-heat cycles which lasted approximately 30 minutes each, the last 10 minutes of which the model was held at a maximum prescribed temperature which ranged from 870 to 1080 K (1100° to 1480° F). Although these radiant-heat cycles supplement those of previous tests (ref. 5), no attempt was made to simulate an aerodynamic heating distribution. Once a prescribed model temperature was reached and desired hypersonic flow conditions were established in the test section, the acoustic baffles were retracted and the model was inserted into the stream for as long as possible. For the angle-of-attack runs the model was pitched up from the horizontal position to the desired angle during insertion into the stream.

RESULTS AND DISCUSSION

Pressure and Heating Distributions

Pressure distributions over the leading edge were essentially uniform across the span with a slight drop in pressure near the fences. The spanwise pressure drop increased with angle of attack to a maximum of 10 percent for $\alpha = 20°$. Typical spanwise pressure distributions for the 20° angle-of-attack test are shown in figure 5. In general, the results indicate that the aerodynamic fences and spanwise extensions were adequate in producing two-dimensional flow over the heat-pipe leading edge and most of the extension area. The experimental and design chordwise pressure distributions are compared in figures 6(a), 6(b), and 6(c) for angles of attack of 0°, 10°, and 20°, respectively. The distributions are in good agreement, as would be expected. The design conditions from reference 4 ($T_{t,c} = 3170$ K (5250° F) and $p_s = 17$ kPa (2.5 psia)) differ somewhat from test conditions in the 8-foot HTST. Therefore, to match the design heat-flux level of 409 kW/m^2 (36 Btu/ft^2-s) (more critical

design criteria), the 8-foot HTST was operated at higher (three to seven times) stagnation pressures.

Experimental pressure distributions and tunnel conditions were input to a boundary-layer computer program (ref. 11) to calculate steady-state aerodynamic heating distributions over the leading edge. Hot-wall values were based on experimentally determined maximum operating temperatures. The calculated and design heat-flux distributions normalized to the corresponding stagnation heat flux are compared in figures 7(a), 7(b), and 7(c) for $\alpha = 0^{\circ}$, 10°, and 20°, respectively. The distributions are in excellent agreement, and the calculated heat flux of the present study was within 3 percent of design level. The heat-flux distributions were integrated and steady-state operating temperatures were calculated using an experimentally determined emissivity of 0.87.

Thermal Response

Typical chordwise temperature histories at three locations, shown in figure 8, indicate that steady-state conditions were reached during preheat and were maintained during the aerothermal test. Also, maximum experimental temperatures and calculated steady-state operating temperatures were in good agreement (as shown in table IV), thereby corroborating steady-state operation and the method for calculating heating rates.

Typical spanwise and chordwise steady-state temperature distributions are presented in figures 9 and 10, respectively. The results shown in figure 9 indicate that spanwise temperature gradients, which existed during the radiant preheat, were essentially eliminated during the aerothermal tests, thereby suggesting that the gradients were the consequence of the nonuniformity of the radiant heating and not the nonuniformity of heat-pipe performance. Specifically, the results shown in figure 10 confirm the results of previous radiant-heat tests (ref. 5) which suggested that the use of heat pipes in cooling a leading edge of hypersonic cruise and space transportation systems is a feasible method for lowering localized stagnation temperatures to allow the use of available and durable superalloys in leading-edge construction. More generally, the results indicate that heat pipes can accommodate very intense localized heating and effectively isothermalize structural components.

Effect of Net Capillary Pumping Head

The net capillary pumping head is the difference between the capillary pumping head (which is a function of the surface tension of the working fluid and the effective pore radius of the wick) and the sum of liquid and vapor frictional losses and the gravitational head. The gravitational head is dependent upon the vertical location of the evaporator (heat input region) and condenser (heat rejection region) sections of the heat pipe and is positive if the evaporator is above the condenser. As explained in reference 5, a wicking limit is encountered when the capillary pumping head is just sufficient to provide the mass-flow rate needed to balance the applied heating rate. If the wicking limit is exceeded, the wick will dryout in the evaporator section (starting at a

point farthest from the condenser section) and the local temperature there will increase rapidly.

Varying the angles of attack and roll varies the net capillary pumping head. In the wind tunnel, increasing the angle of attack lowers the wicking limit by increasing the gravitational pressure head and increasing the flow length, hence frictional losses. Increased pressure head and flow length result from the movement of the stagnation region farther down the lower surface. Rolling the model 90° eliminates the pressure head due to gravity and thereby increases the wicking limit.

Theory indicates that steady-state heat-pipe performance will not be adversely affected by changes in the net capillary pumping head provided that the wicking limit is not exceeded. Chordwise temperature distributions along a centrally located heat pipe are shown in figure 10 for various angles of attack and roll. Results of the present study and previous tests of the leading edge (ref. 5) show that changes in the net capillary pumping head and heating distributions as a result of the variations in angles of attack and roll had no noticeable effect on heat-pipe performance. Exceeding the wicking limit did, however, inhibit performance and is discussed in a subsequent section.

Durability

The aerothermal tests of the present study demonstrated the durability of the leading edge in withstanding aerodynamic heating and pressure loads equivalent to and in excess of design requirements (refs. 3 and 4). Some unexpected events in the present investigation also demonstrated overdesign performance of the heat-pipe leading edge. These events are significant because they demonstrate the tolerance of the heat-pipe leading edge to adverse effects that might otherwise be considered deleterious from a structural standpoint.

Dryout during radiant preheating.- Prior to the 0° roll test (test 3) several radiant preheat checkout tests were conducted to determine whether one heater would be sufficient in starting the heat pipes from the frozen state. (As explained in ref. 5, during a normal heat-pipe startup from the frozen state, a constant temperature continuum region develops at the evaporator and grows until it reaches the ends of the heat pipe or stops short of the ends of the heat pipe because of some lower than design heating condition.) Chordwise temperature distributions at various times for one such checkout test (fig. 11), with a single heater located as shown by the sketch, indicate that local dryout of the wick in the evaporator region ($l/l_T \cong 1.0$) caused temperatures there to rise to over 1300 K (1900° F). Results indicate that the region of dryout grew from the evaporator section toward the condenser section of the heat pipe (which in this particular configuration is toward the nose and lower surface).

Wick dryout is attributed to the decrease in net capillary pumping head caused by frictional and gravitational pressure losses. The net capillary pumping head decreased as the continuum region grew (from the upper to the lower surface) until a wicking limit, shown in figure 12 for heater configuration 1, was exceeded. During startup from the frozen state, the temperature of the heat

pipes rises along the sonic limit curve until the heat pipes are fully operational (refs. 1, 5, and 12). As shown in figure 12, for heater configuration 2 (ref. 5) the heat pipes exceeded the maximum operating point for configuration 1 but were below the wicking limit for configuration 2 and, hence, did not experience dryout. For heater configuration 1, however, the wicking limit was lower and was probably exceeded, thus causing dryout. For subsequent tests, configuration 1 was modified by adding an array of heaters below the lower surface of the leading edge, and startup of all heat pipes occurred normally.

Thermal buckling.- The side extensions constrained the lateral expansion of the leading edge, thereby causing local buckling (fig. 13) in the aerodynamic skin between the heat pipes. (See fig. 1.) The overtemperature, as a result of exceeding the wicking limit, caused more pronounced buckling in the upper aft section of the leading edge. However, the structural integrity of the model was not compromised, as indicated by the successful completion of the remaining six aerothermal tests.

Erosion damage.- Contaminants in the test stream (inevitable in high-speed true-temperature wind tunnels) of the 8-foot HTST caused some erosion damage to the leading-edge model. After two aerothermal tests the nose section of the model was pitted and the zirconium coating on the extensions was severely eroded as shown in figure 14. The thin, Hastelloy X skin (0.051 cm (0.02 in.)) of the heat-pipe leading edge suffered minor damage with no particle penetration. However, the high-emissivity ceramic paint eroded away near the nose and exposed the metal surface to oxidation by the airstream. Oxidation of the metal surface could have reduced the emissivity and increased the heat absorbed. The extensions were resurfaced for subsequent tests.

CONCLUDING REMARKS

A sodium-filled, Hastelloy X, heat-pipe-cooled leading edge, which had previously withstood 9 radiant-heat tests, was subjected to 8 aerothermal tests and 25 supplemental radiant-heat cycles. The later radiant-heat cycles were required to assure proper startup of all heat pipes and to establish steady-state heat-pipe operation during the aerothermal tests. During the aerothermal tests the model experienced realistic Earth-entry aerothermal heating and pressure loads in the Langley 8-foot high-temperature structures tunnel at a nominal Mach number of 7. The heat-pipe leading-edge model with a span of 15 cm (6 in.) was sting mounted in the tunnel with spanwise extensions and aerodynamic fences attached to each side of the model to produce a two-dimensional flow field. The model was tested at angles of attack of 0°, 10°, and 20°, angles of roll of 0° and 90°, calculated model stagnation heating rates ranging from 244 to 422 kW/m^2 (21.5 to 37.2 Btu/ft^2-s), and nominal model stagnation pressures of about 50 and 124 kPa (7.3 and 18 psia).

The heat pipes operated isothermally for these test conditions with maximum operating temperatures ranging from 950 to 1100 K (1250° to 1520° F). Near steady-state temperatures obtained during the aerothermal tests were in good agreement with analytical results. The pressure and heat-flux distributions were also in good agreement with design distributions.

Heat-pipe performance was not affected by variations in the net capillary pumping head due to gravitational and frictional pressure losses caused by variations in angles of attack and roll. The capillary pumping or wicking limit was exceeded, however, during a radiant preheat cycle, and temperatures in the region of wick dryout exceeded 1300 K (1900° F). Some local buckling occurred in the aerodynamic skin between heat pipes because of the overtemperature and the lateral constraint of the side extensions; however, the buckling did not affect heat-pipe performance or compromise the structural integrity of the model. Impingement of particles, which was severe enough to erode the zirconium coating from the spanwise extensions, caused only minor damage to the Hastelloy X skin of the heat-pipe model.

Results of the study indicate that the heat-pipe-cooled leading edge performed well in a realistic aerothermal environment and demonstrated overdesign capability as well. Specifically, results of the aerothermal and previous radiant-heat tests suggest that the use of the heat pipes in cooling a leading edge of hypersonic cruise and space transportation systems is a feasible method for lowering localized stagnation temperatures to allow the use of available and durable superalloys in leading-edge construction. More generally, the results indicate that the heat pipes can accommodate very intense localized heating and effectively isothermalize structural components.

Langley Research Center
National Aeronautics and Space Administration
Hampton, VA 23665
September 27, 1978

APPENDIX

7-INCH MACH 7 PILOT TUNNEL TESTS

The 7-inch Mach 7 pilot tunnel at the Langley Research Center is a 1/12.7-scale facility of the 8-foot HTST with similar flow characteristics, thus permitting studies of flow and blockage characteristics of models to be tested in the 8-foot HTST. Flow-blockage and oil-flow studies in the 7-inch Mach 7 pilot tunnel qualitatively assessed the spanwise uniformity of flow over the heat-pipe model with and without side extensions and fences. The results were used to determine the maximum size extensions which could be accommodated by the facility without causing flow breakdown. In addition to producing a two-dimensional flow field over the model, the extensions also provide an instrumented surface for measuring pressure and heating conditions imposed on the leading edge during the 8-foot HTST tests. As shown in figure 15, three models were used (spans of 1.3, 3.8, and 6.4 cm (0.5, 1.5, and 2.5 in.)) to depict the leading edge without extensions, the leading edge plus two extensions equal in span to the leading edge, and the leading edge plus two extensions twice the span of the leading edge. Results from the shorter span models indicated that the best flow patterns would be obtained with the maximum span. However, because of tunnel-blockage problems at an angle of attack of 20°, the 6.35-cm (2.5-in.) span model had to be shortened to 5.72 cm (2.25 in.). Oil-flow patterns over the leeward and windward surfaces of the 5.72-cm (2.25-in.) span model for angles of attack of 0°, 10°, and 20°, with and without aerodynamic fences, are shown in figures 16 and 17, respectively, for a combustor total temperature of 1855 K (3340° R), a free-stream Mach number of 6.76, a free-stream dynamic pressure of 49.80 kPa (1040 lbf/ft^2), and a free-stream unit Reynolds number of 3.77×10^6 per m (1.15×10^6 per ft).

Results were similar to those obtained on a flat plate (ref. 10) and exhibit the need for aerodynamic fences to straighten the flow over the surface of the model, thereby preventing outflow over the sides of the windward surface and inflow over the sides of the leeward surface of the model at angles of attack. Results of these tests indicated that the maximum span of the 8-foot HTST model should be limited to 68.8 cm (27 in.) and aerodynamic fences would be necessary to insure two-dimensional flow.

REFERENCES

1. Silverstein, Calvin C.: A Feasibility Study of Heat-Pipe-Cooled Leading Edges for Hypersonic Cruise Aircraft. NASA CR-1857, 1971.

2. Niblock, G. A.; Reeder, J. C.; and Huneidi, F.: Four Space Shuttle Wing Leading Edge Concepts. J. Spacecr. & Rockets, vol. 11, no. 5, May 1974, pp. 314-320.

3. Study of Structural Active Cooling and Heat Sink Systems for Space Shuttle. Rep. No. MDC E0638 (Contract No. NAS 8-27708), McDonnell Douglas Astronautics Co. - East, June 30, 1972. (Available as NASA CR-123912.)

4. Design, Fabrication, Testing, and Delivery of Shuttle Heat Pipe Leading Edge Test Modules. Volume II - Technical Report. Rep. MDC E0775, McDonnell Douglas Astronautics Co., Apr. 1973. (Available as NASA CR-138673.)

5. Camarda, Charles J.: Analysis and Radiant Heating Tests of a Heat-Pipe-Cooled Leading Edge. NASA TN D-8468, 1977.

6. Leyhe, E. W.; and Howell, R. R.: Calculation Procedure for Thermodynamic, Transport, and Flow Properties of the Combustion Products of a Hydrocarbon Fuel Mixture Burned in Air With Results for Ethylene-Air and Methane-Air Mixtures. NASA TN D-914, 1962.

7. Howell, R. R.; and Hunt, L. R.: Methane - Air Combustion Gases as an Aerodynamic Test Medium. J. Spacecr. & Rockets, vol. 9, no. 1, Jan. 1972, pp. 7-12.

8. Hunt, L. Roane: Aerodynamic Force and Moment Characteristics of Spheres and Cones at Mach 7.0 in Methane-Air Combustion Products. NASA TN D-2801, 1965.

9. Weinstein, Irving: Heat-Transfer and Pressure Distributions on Hemisphere-Cylinders in Methane-Air Combustion Products at Mach 7. NASA TN D-7104, 1973.

10. Deveikis, William D.; and Hunt, L. Roane: Loading and Heating of a Large Flat Plate at Mach 7 in the Langley 8-Foot High-Temperature Structures Tunnel. NASA TN D-7275, 1973.

11. Grose, Ronald D.; and Kendall, Robert M.: A Nonsimilar Solution for Laminar and Turbulent Boundary Layer Flows Including Entropy Layers and Transverse Curvature. NASA CR-73481, 1970.

12. Cotter, T. P.: Heat Pipe Startup Dynamics. Heat Pipes, Volume XVI of AIAA Selected Reprint Series, Chang-Lin Tien, ed., Sept. 1973, pp. 42-45.

TABLE I.- THERMOCOUPLE LOCATIONS

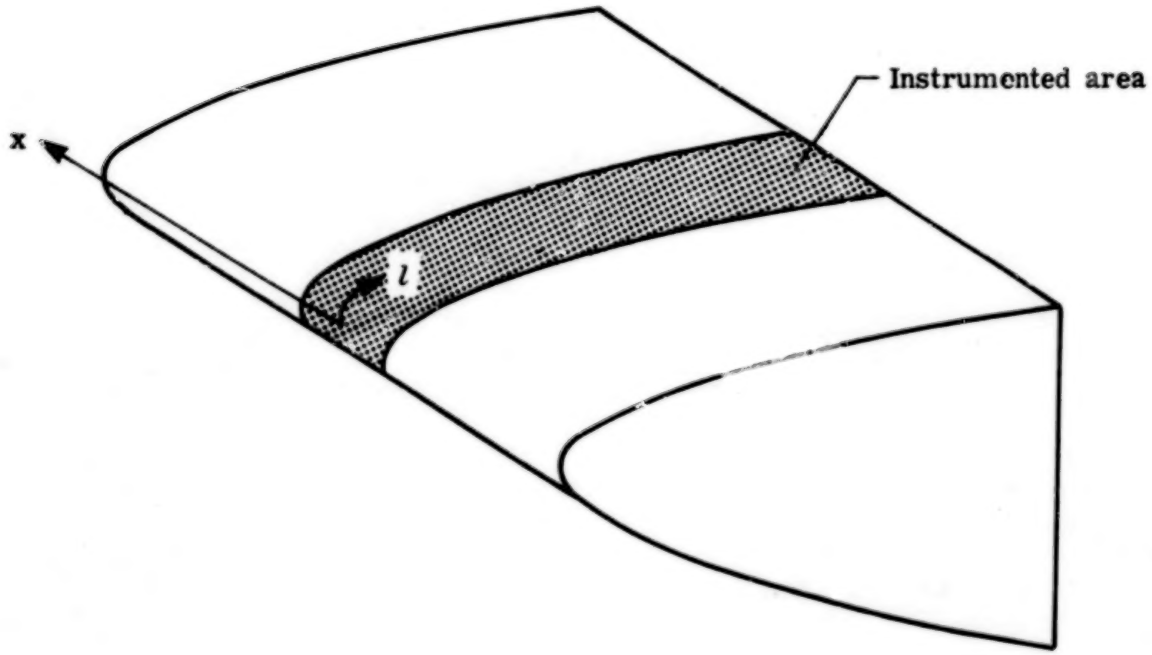

Thermocouple designation	x		l (a)		Thermocouple designation	x		l (a)	
	cm	in.	cm	in.		cm	in.	cm	in.
1	-0.64	-0.25	3.05	1.2	19	3.18	1.25	-3.05	-1.2
2	↓	↓	6.1	2.4	20	1.91	.75	↓	↓
3	↓	↓	10.41	4.1	21	-.64	-.25	↓	↓
4	↓	↓	13.46	5.3	22	-3.18	-1.25	↓	↓
5	↓	↓	24.26	9.55	23	-4.45	-1.75	↓	↓
6	↓	↓	33.27	13.1	24	-5.72	-2.25	↓	↓
7	↓	↓	43.15	16.99	25	-6.99	-2.75	↓	↓
8	↓	↓	51.23	20.17	26	6.99	2.75	51.23	20.17
9	↓	↓	-6.1	-2.4	27	4.45	1.75	↓	↓
10	↓	↓	-10.41	-4.1	28	1.91	.75	↓	↓
11	↓	↓	-13.46	-5.3	29	-3.18	-1.25	↓	↓
12	↓	↓	-24.26	-9.55	30	-5.72	-2.25	↓	↓
13	↓	↓	-35.05	-13.8	31	6.99	2.75	-51.23	-20.17
14	↓	↓	-43.15	-16.99	32	4.45	1.75	↓	↓
15	↓	↓	-51.23	-20.17	33	1.91	.75	↓	↓
16	6.99	2.75	-3.05	-1.2	34	-3.18	-1.25	↓	↓
17	5.72	2.25	↓	↓	35	-5.72	-2.25	↓	↓
18	4.45	1.75	↓	↓					

[a]Measured from nose along inside surface of heat pipes.

TABLE II.- PRESSURE-ORIFICE LOCATIONS

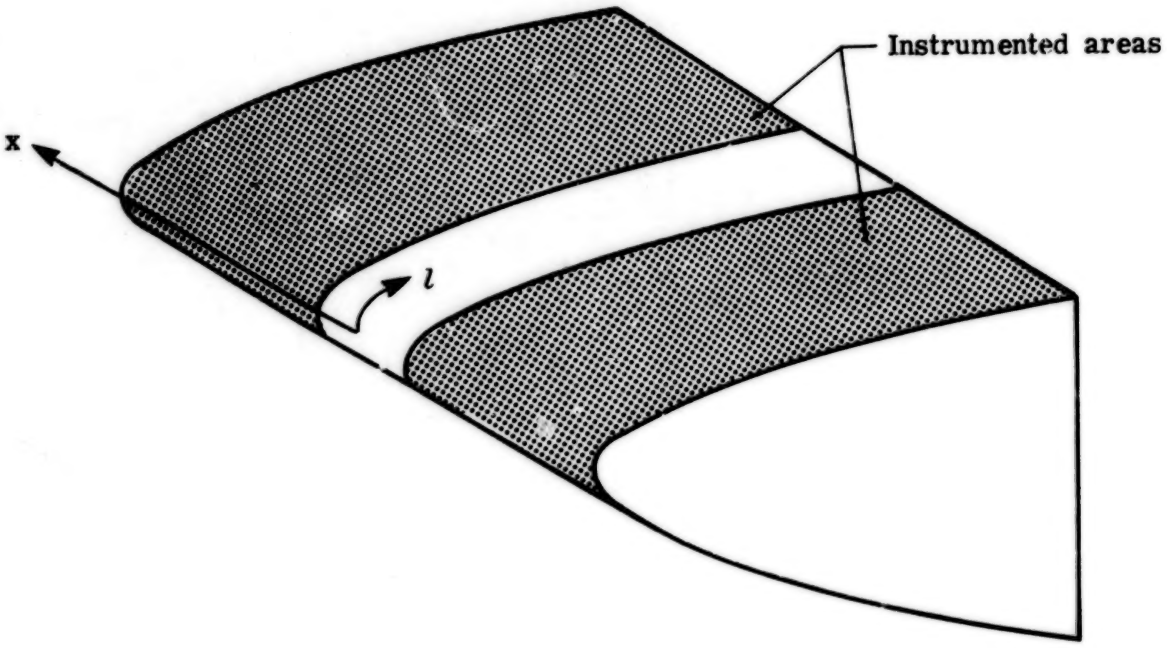

Pressure-orifice designation	x		l		Pressure-orifice designation	x		l	
	cm	in.	cm	in.		cm	in.	cm	in.
1	10.16	4.0	50.8	20	15	10.16	4.0	-20.32	-8
2	↓	↓	30.48	12	16	↓	↓	-30.48	-12
3	↓	↓	20.32	8	17	↓	↓	-50.8	-20
4	↓	↓	12.7	5	18	20.32	8.0	50.8	20
5	↓	↓	7.62	3	19	↓	↓	20.32	8
6	↓	↓	5.08	2	20	↓	↓	0	0
7	↓	↓	2.54	1	21	↓	↓	-20.32	-8
8	↓	↓	1.27	.5	22	↓	↓	-50.8	-20
9	↓	↓	0	0	23	-20.32	-8.0	50.8	20
10	↓	↓	-1.27	-.5	24	↓	↓	20.32	8
11	↓	↓	-2.54	-1	25	↓	↓	0	0
12	↓	↓	-5.08	-2	26	↓	↓	-20.32	-8
13	↓	↓	-7.62	-3	27	↓	↓	50.8	-20
14	↓	↓	-12.7	-5					

TABLE III.- TEST CONDITIONS

Test	$T_{t,c}$		p_∞		M_∞	q_∞		R_∞		α, deg	ϕ, deg	p_s	
	K	°R	kPa	psia		kPa	lbf/ft^2	per m	per ft			kPa	psia
1	1829	3260	0.8094	0.1174	6.9	26.8	560	1.82×10^6	0.557×10^6	0	90	50.9	7.38
2	2101	3750	.6481	.0940	7.3	25.3	528	1.68	.513	0	90	50.7	7.35
3	2056	3670	.6757	.0980	7.2	24.6	513	1.71	.52	0	0	47.5	6.89
4	1865	3325	2.111	.3062	6.7	61.9	1293	4.4	1.34	0	0	125.8	18.24
5	2101	3750	1.828	.2652	7.06	52.6	1099	3.58	1.09	10	0	123.2	17.87
6	1962	3500	2.033	.2948	6.8	66.2	1382	4.43	1.35	20	0	119.6	17.34
7	1934	3450	2.048	.2970	6.8	68.3	1426	4.56	1.39	10	0	123.8	17.95
8	1906	3400	2.075	.3010	6.8	62.3	1300	4.56	1.39	0	90	126.2	18.3

TABLE IV.- SUMMARY OF TEST RESULTS

Test	Preheat temp.		Max. operating temp. (exp.)		Max. chordwise ΔT		Hot-wall $\dot{q}_s$		Cold-wall $\dot{q}_s$		Calculated steady-state operating temp.		Time in stream
	K	°F	K	°F	K	°F	kW/m^2	Btu/ft^2-s	kW/m^2	Btu/ft^2-s	K	°F	sec
1	925	1205	950	1250	25	45	261.5	23.04	412.1	36.31	974	1294	32.3
2	875	1115	950	1250	50	90	259.8	22.89	401.2	35.35	972	1290	43.25
[a]3	950	1250	955	1259	7	12.6	243.5	21.46	388.9	34.27	957	1263	52.35
4	1052	1434	1070	1466	.5	.9	422.3	37.21	645.3	56.86	1098	1517	19.98
5	1040	1412	1075	1475	.5	.9	329.6	29.04	617.6	54.42	1041	1414	22.49
6	1075	1475	1100	1520	.5	.9	324.7	28.61	623.8	54.97	1024	1402	16.75
7	890	1142	970	[b]1286	.7	1.3	389.6	34.33	636.1	56.05	1085	1494	31.0
8	1040	1412	1065	1457	1.0	1.8	360.4	31.76	644.4	56.78	1055	1440	23.87

[a]New thermocouples installed.
[b]Steady state not reached.

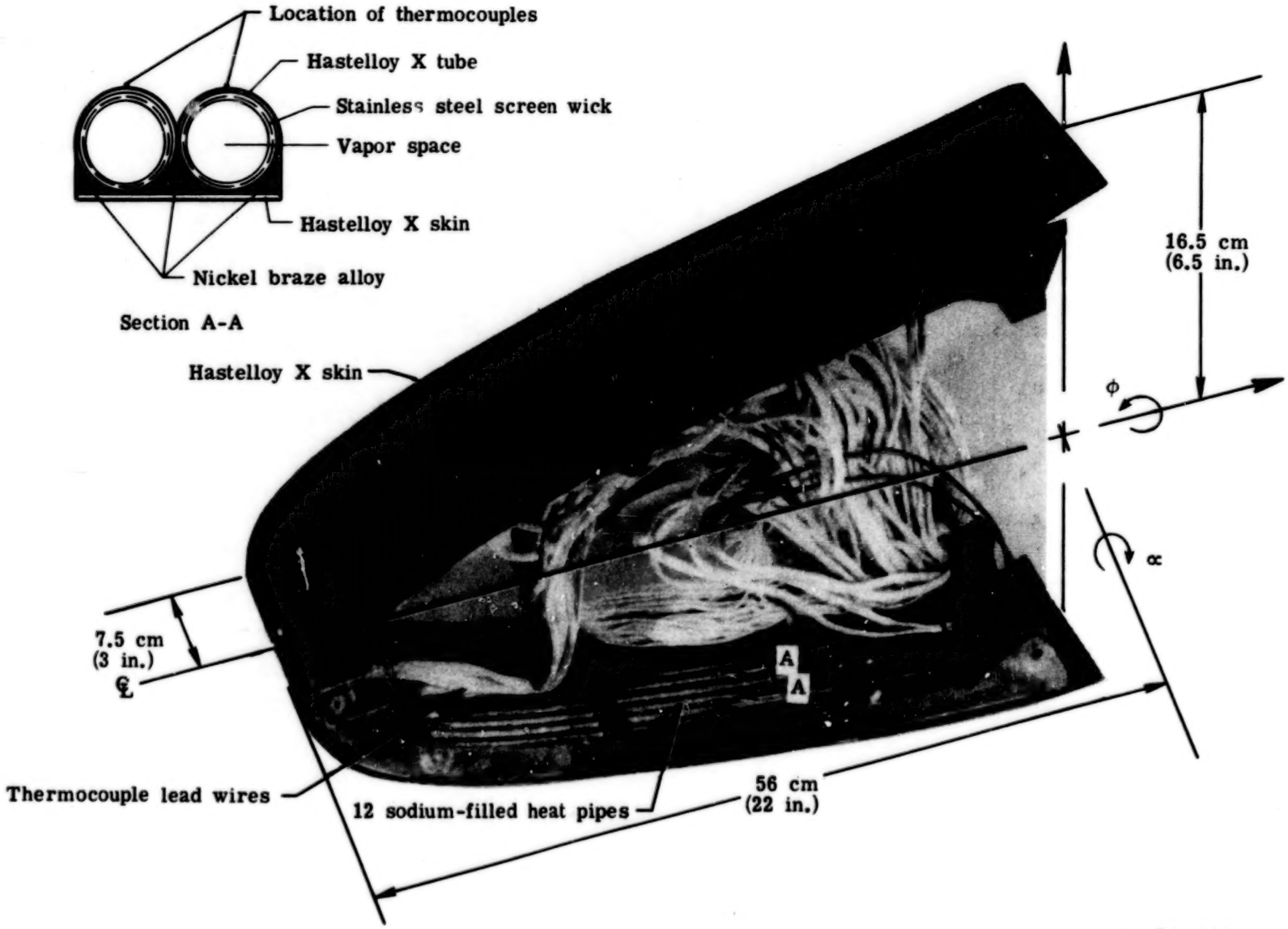

L-74-6010.2

Figure 1.- Heat-pipe-cooled leading-edge test model.

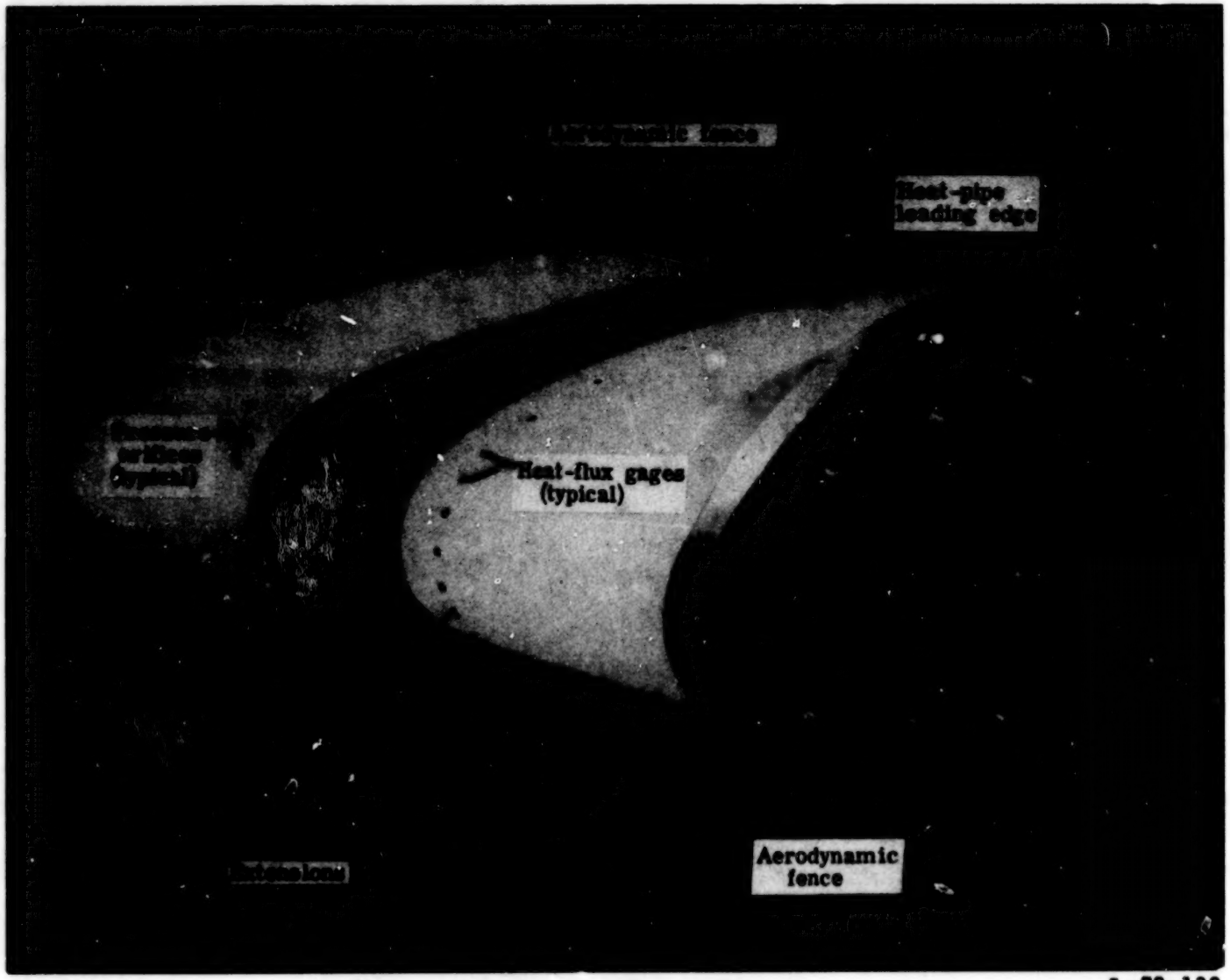

L-78-138

Figure 2.- Wind-tunnel model.

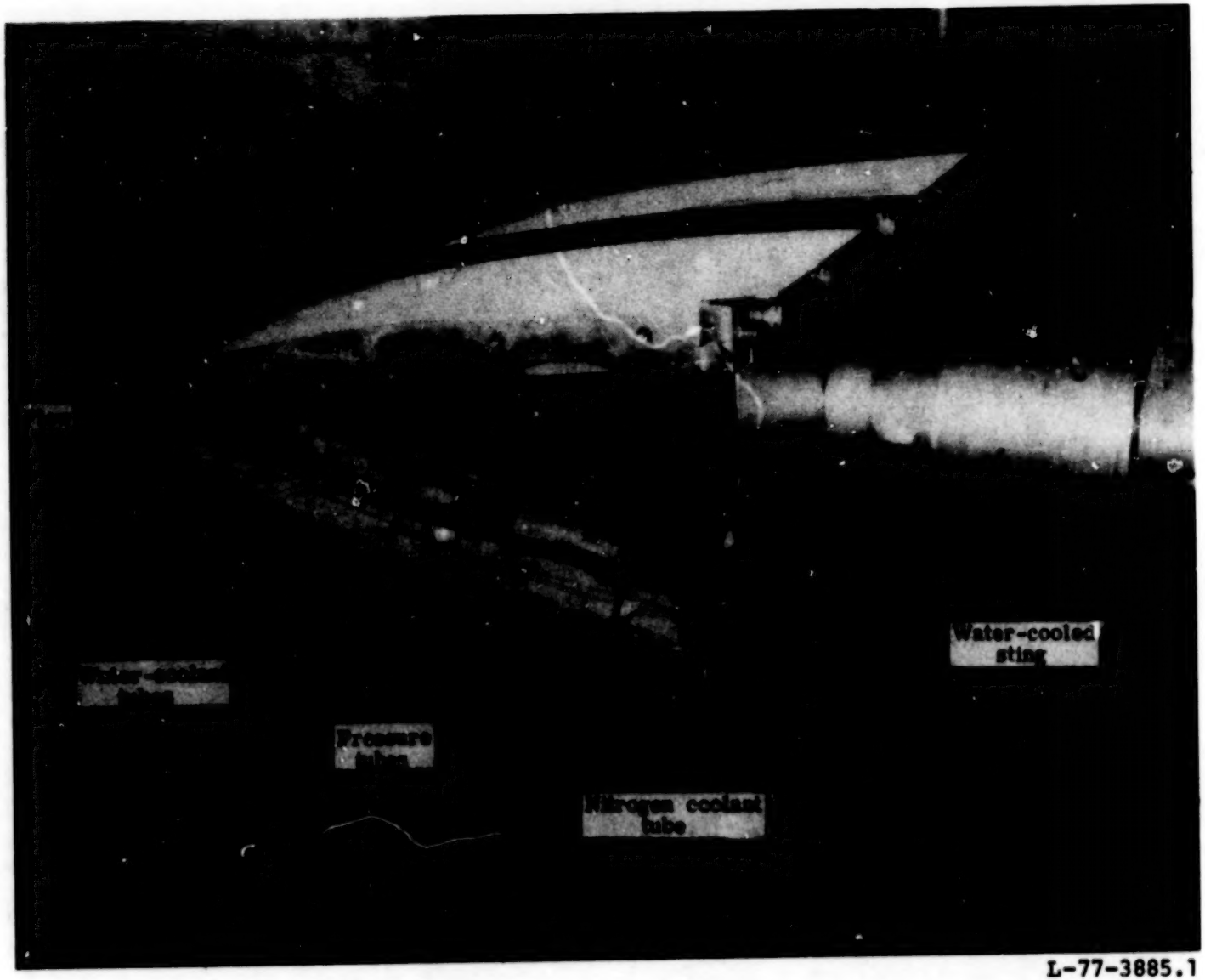

L-77-3885.1

Figure 3.- Instrumented extension section.

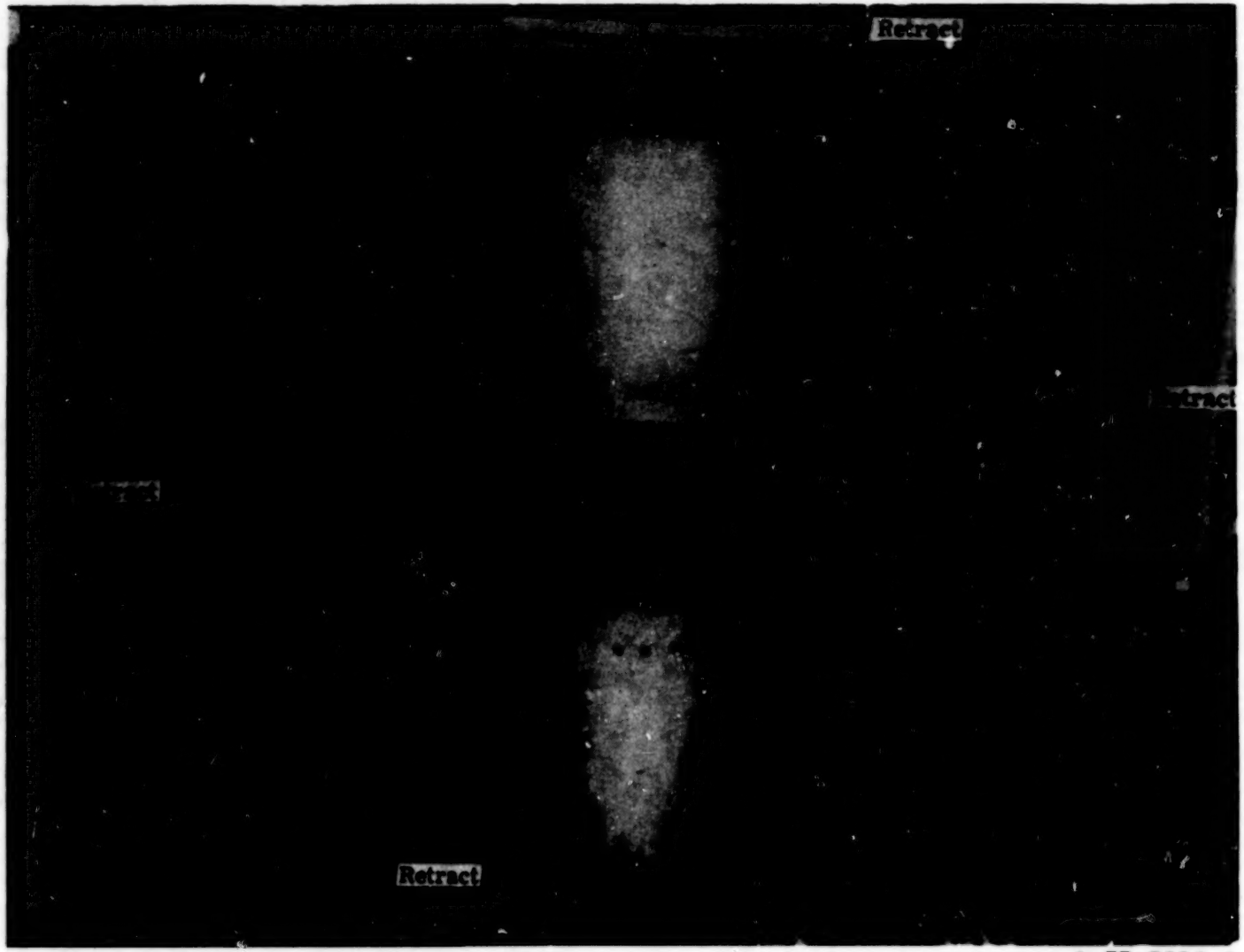

L-77-7010.1

Figure 4.- Retractable radiant heaters in pod section of Langley 8-foot HTST. (Model is in 90° roll position.)

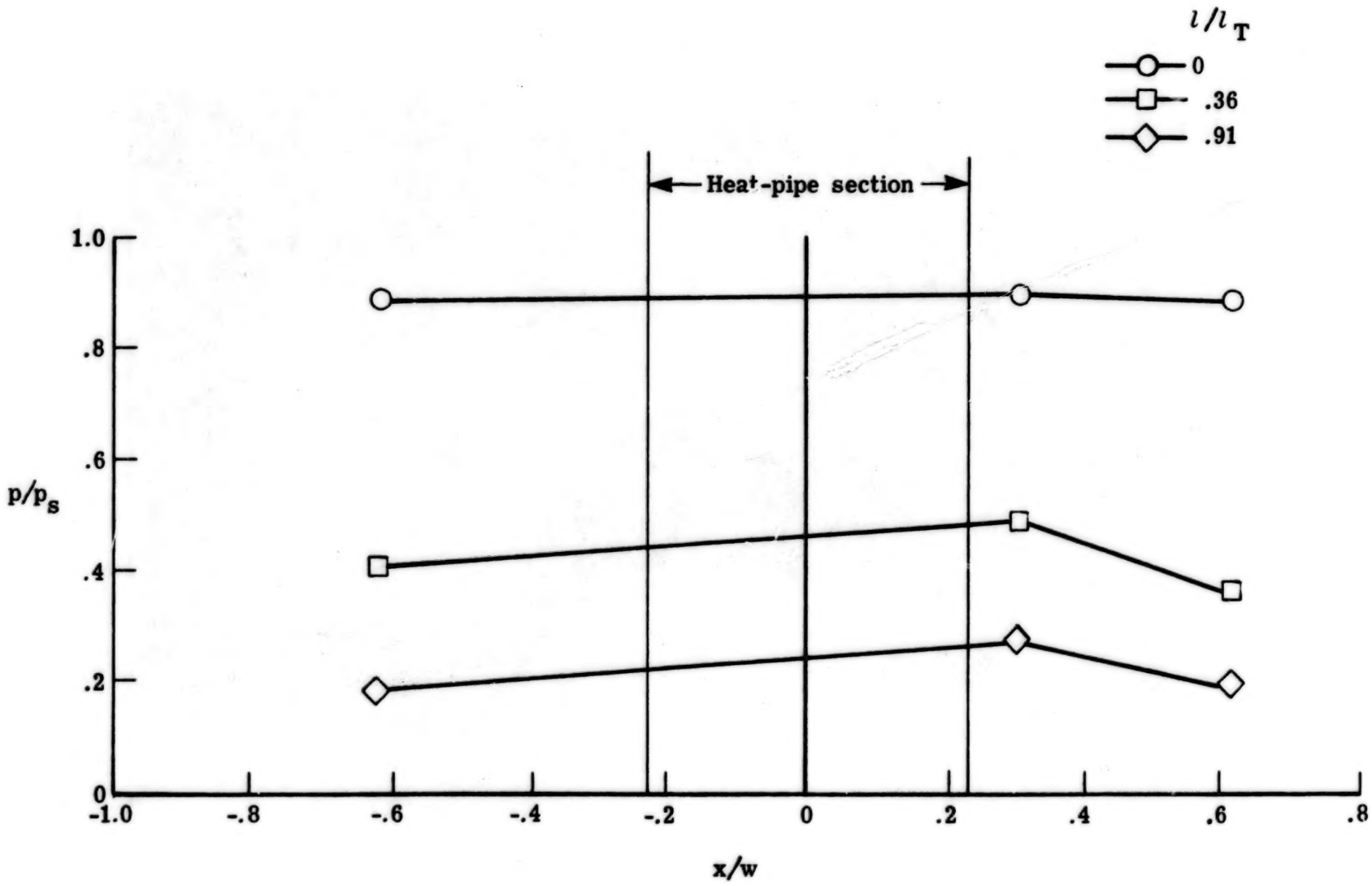

Figure 5.- Normalized spanwise pressure distribution for $\alpha = 20^{o}$ and $p_s = 119.6$ kPa (17.34 psia) at $x/w = 0.308$ (test 6).

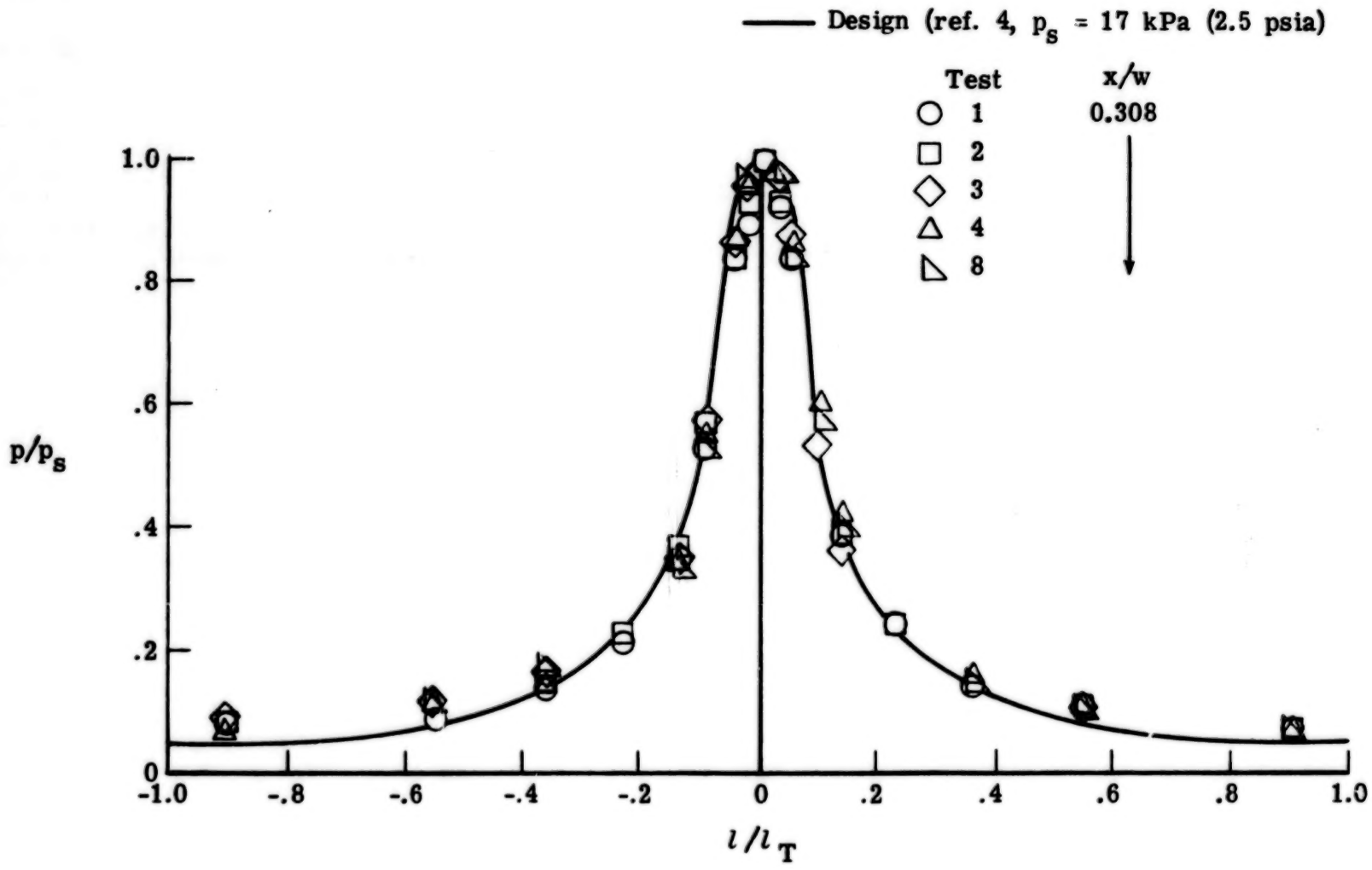

(a) $\alpha = 0^{\circ}$.

Figure 6.- Normalized chordwise pressure distribution.

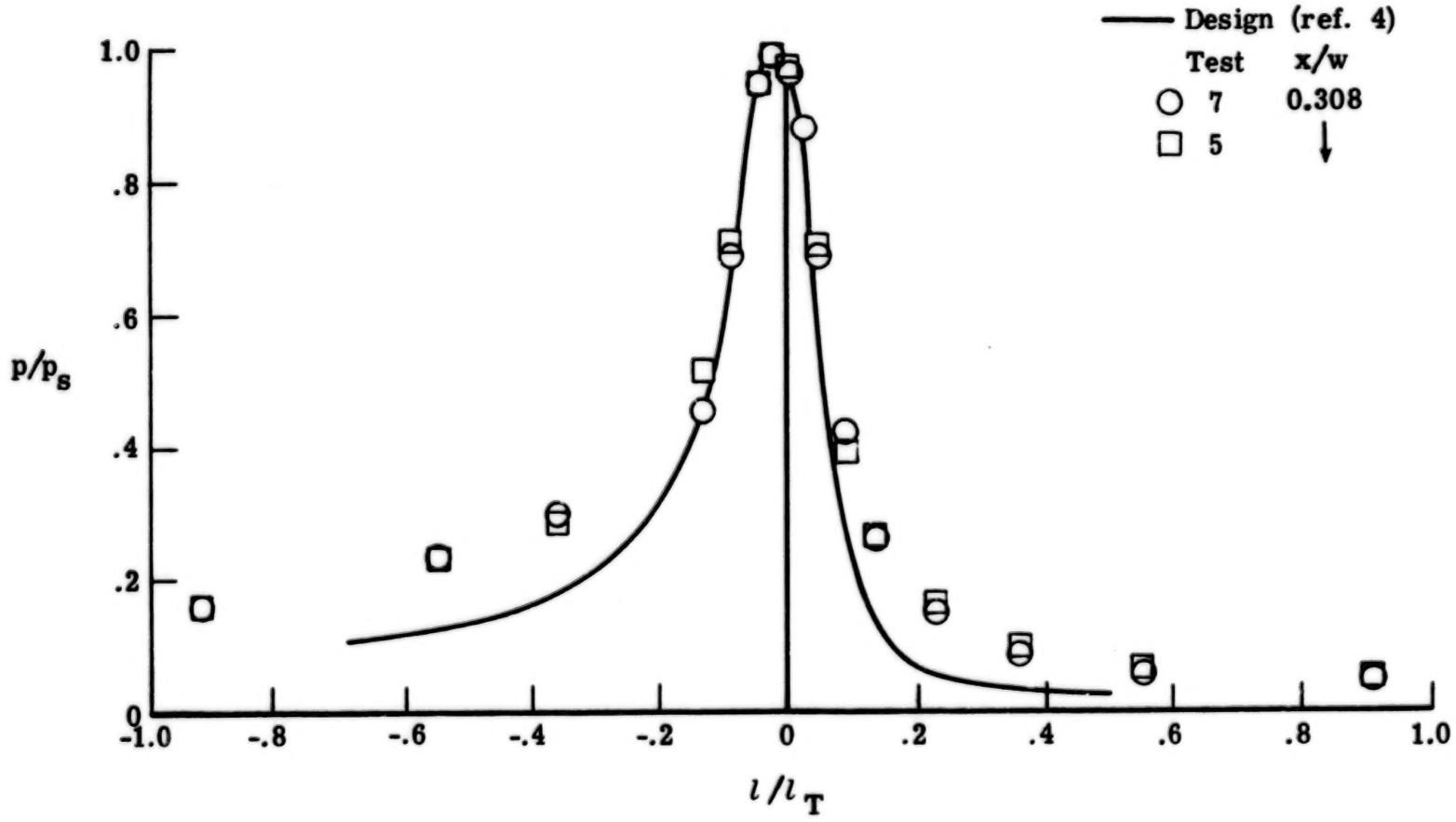

(b) $\alpha = 10^{\circ}$.

Figure 6.- Continued.

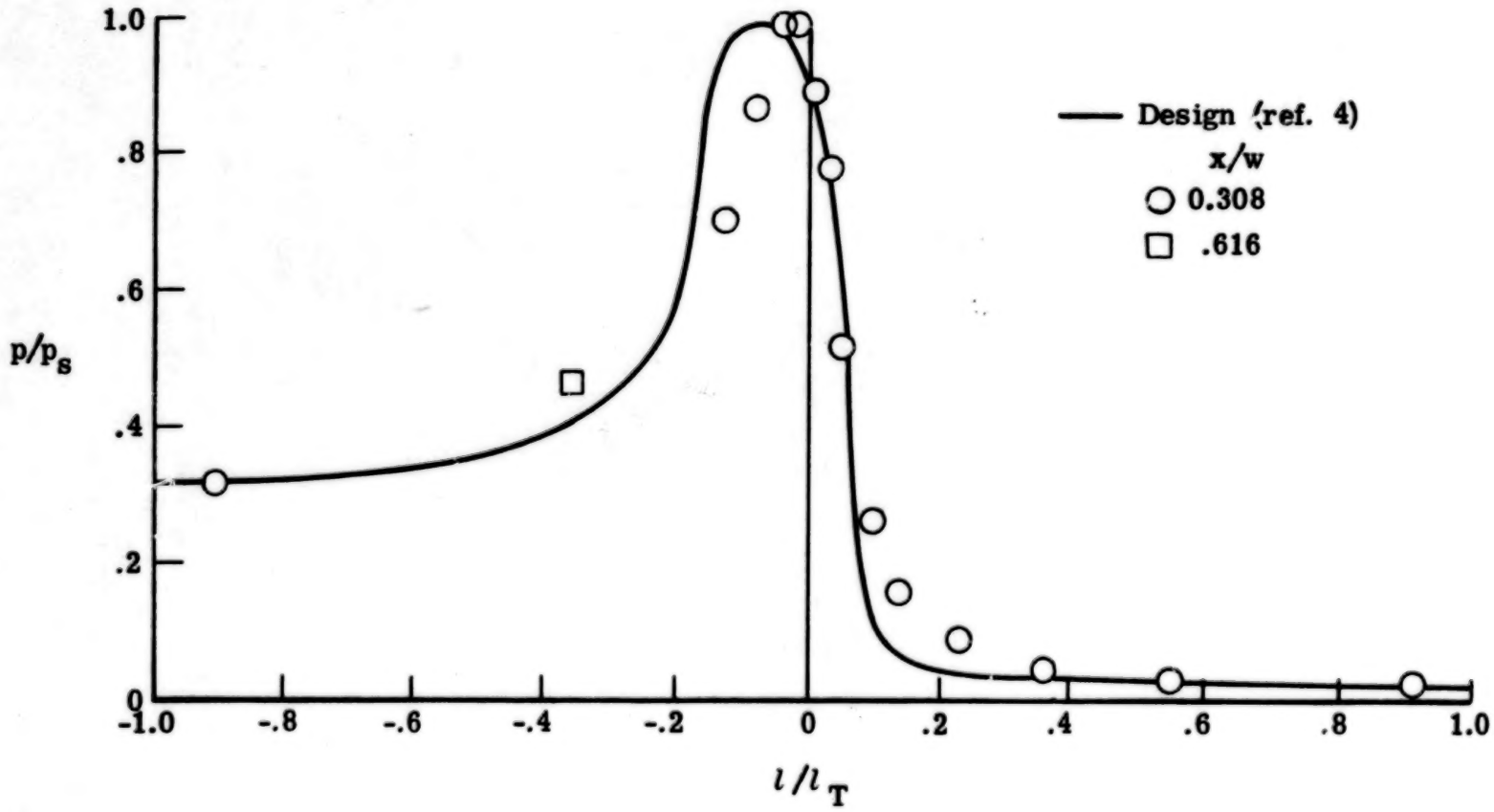

(c) $\alpha = 20^{\circ}$; test 6.

Figure 6.- Concluded.

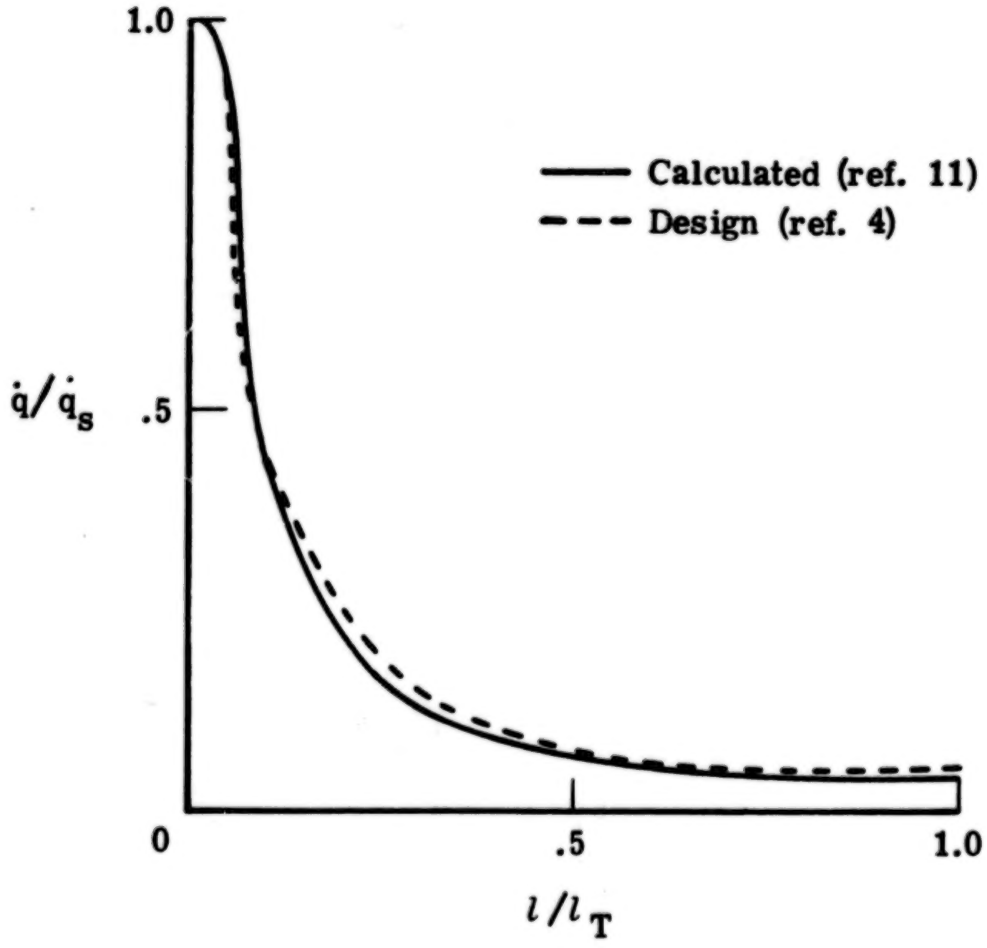

(a) $\alpha = 0^{\circ}$.

Figure 7.- Aerodynamic heating distribution.

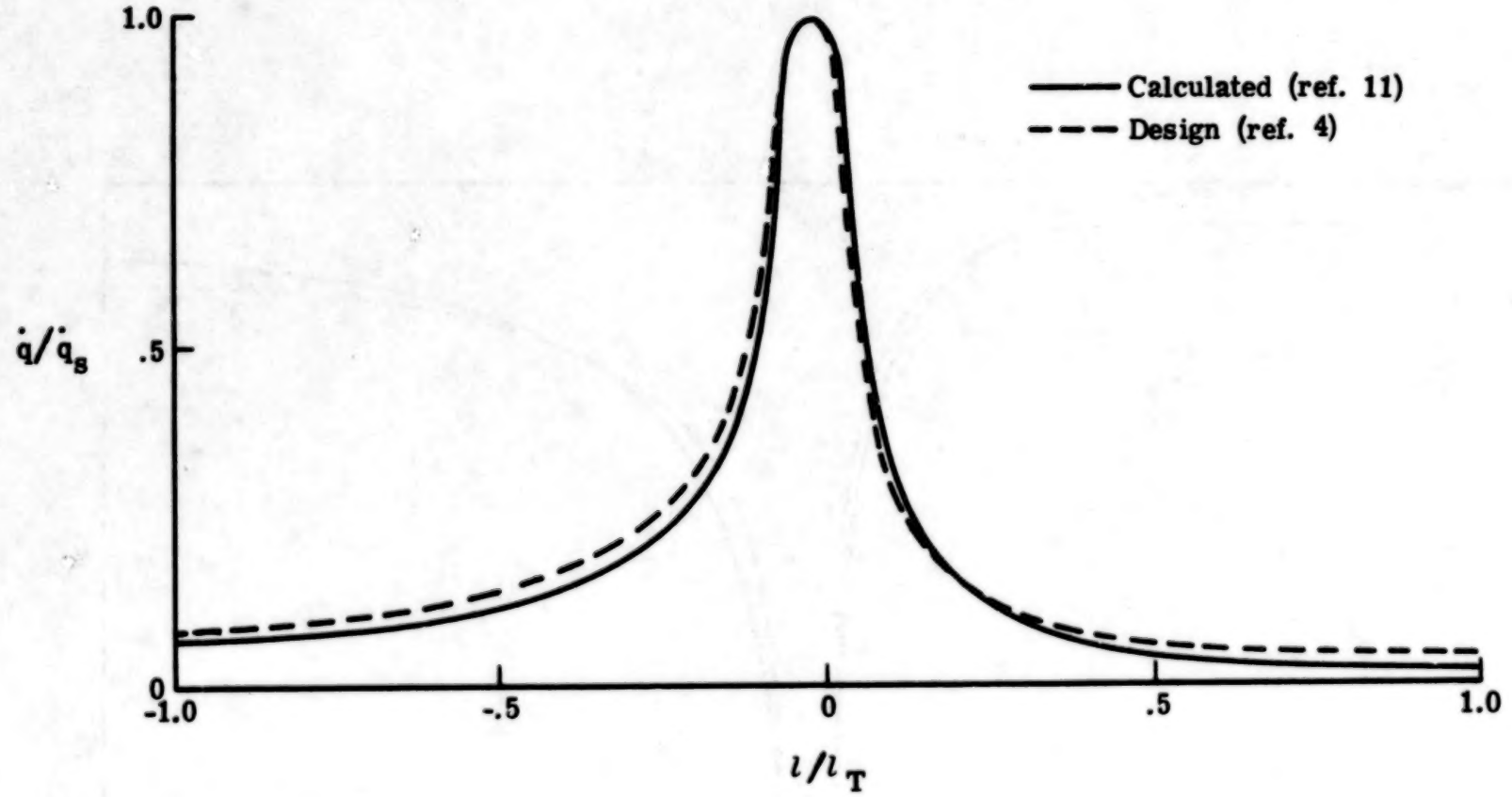

(b) $\alpha = 10^{\circ}$.

Figure 7.- Continued.

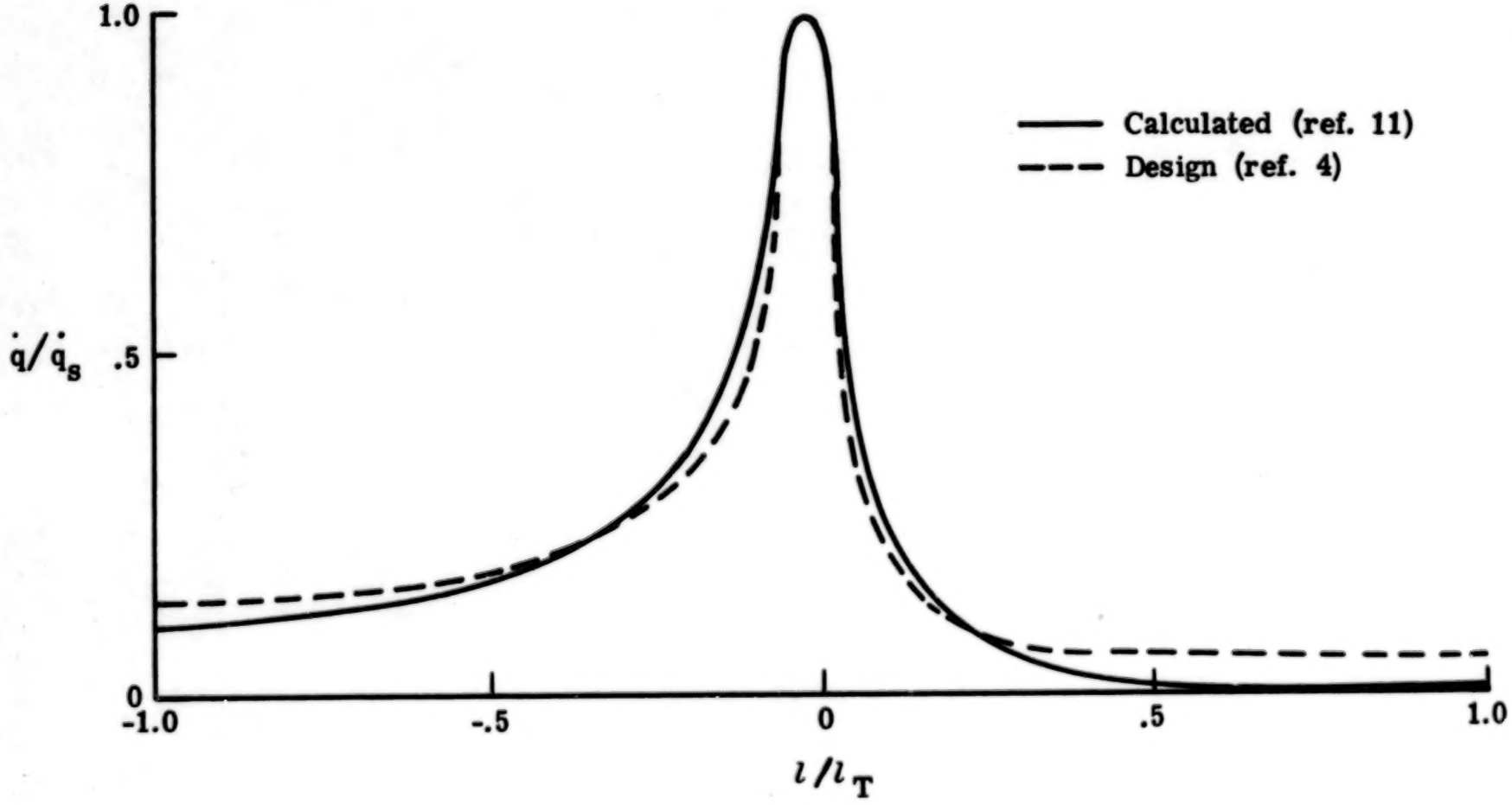

(c) $\alpha = 20^{\circ}$.

Figure 7.- Concluded.

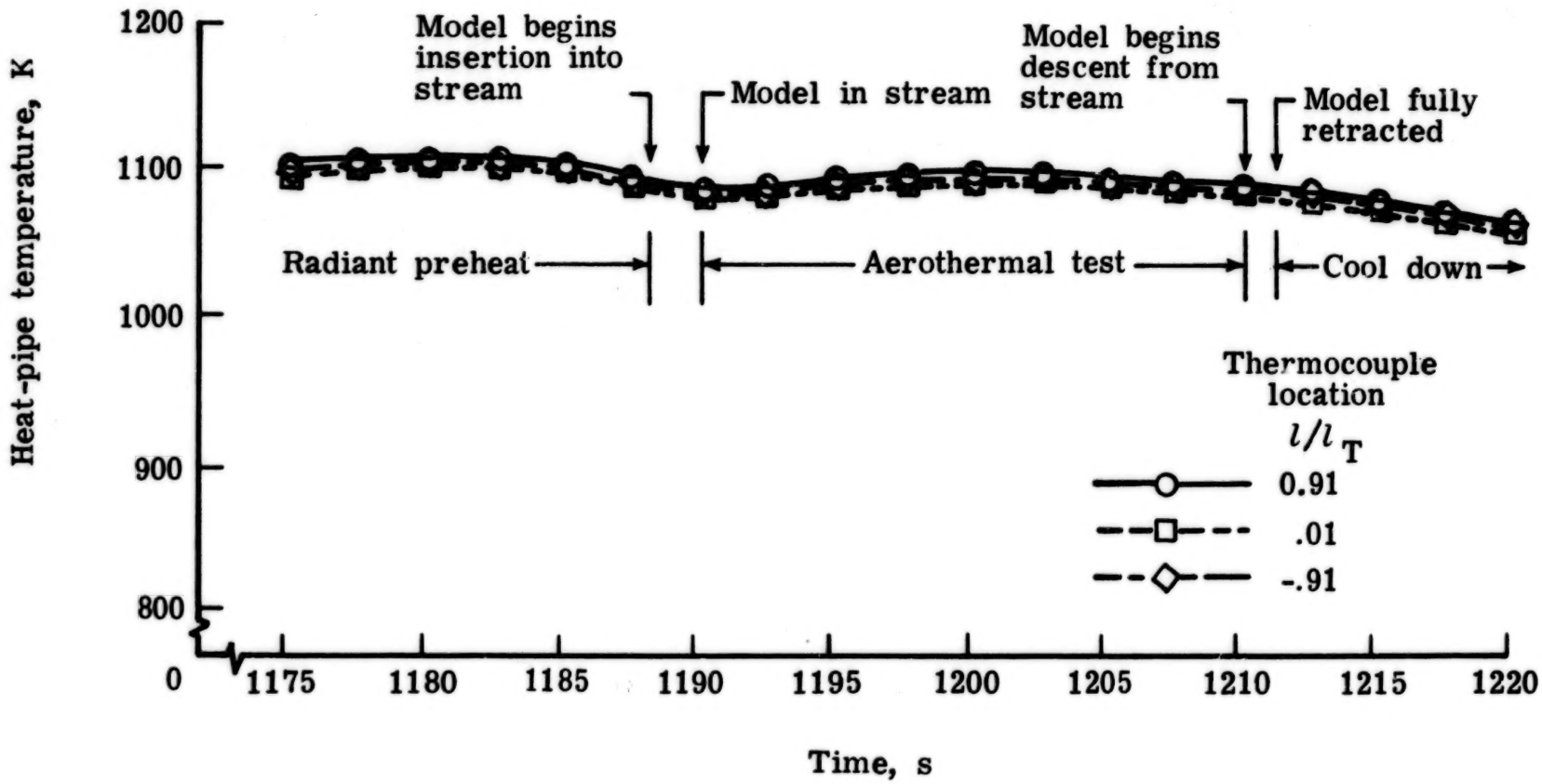

Figure 8.- Typical temperature histories at various locations along centrally located heat pipe. (x/w = -0.02) (test 4).

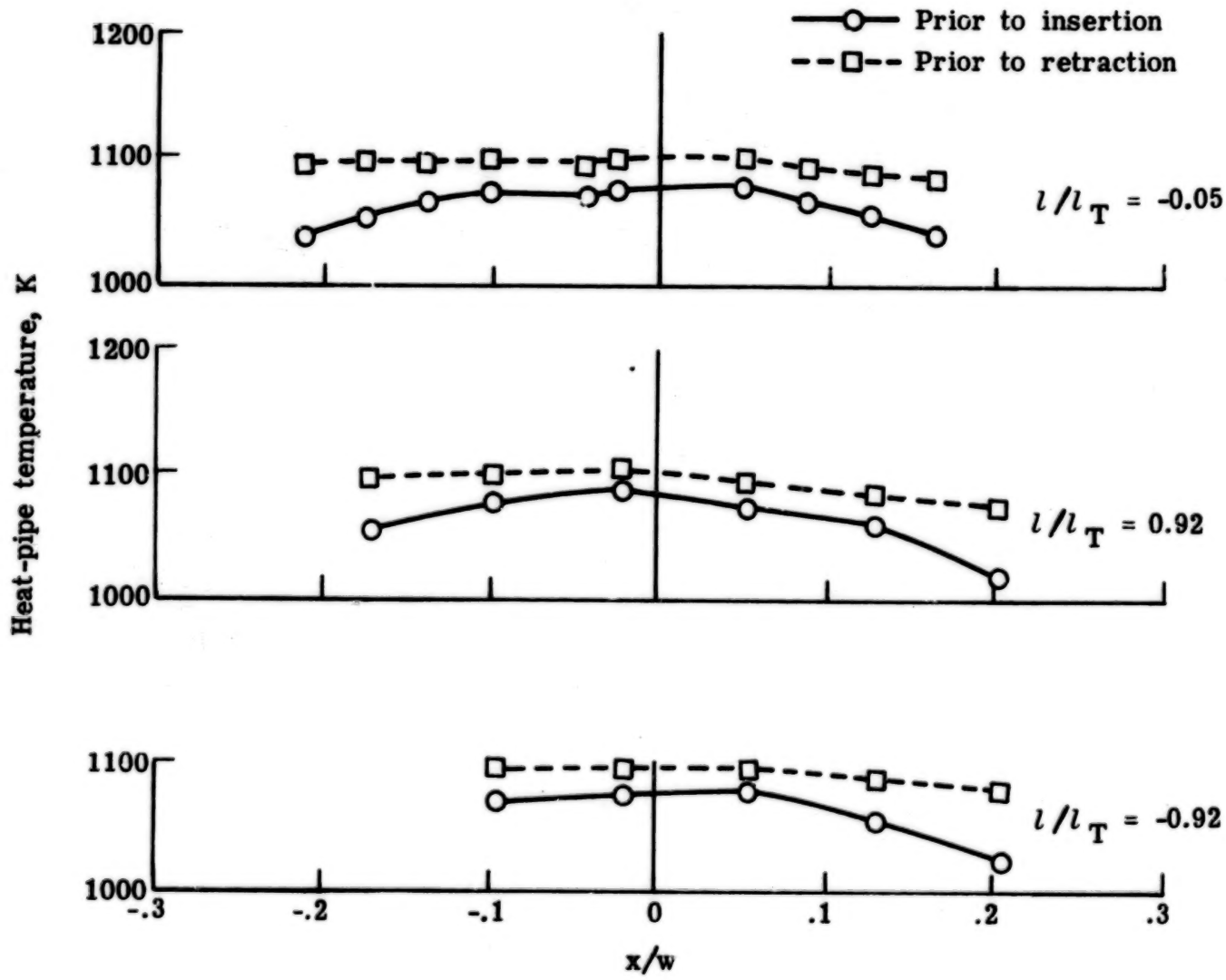

Figure 9.- Typical spanwise temperature distributions (test 6).

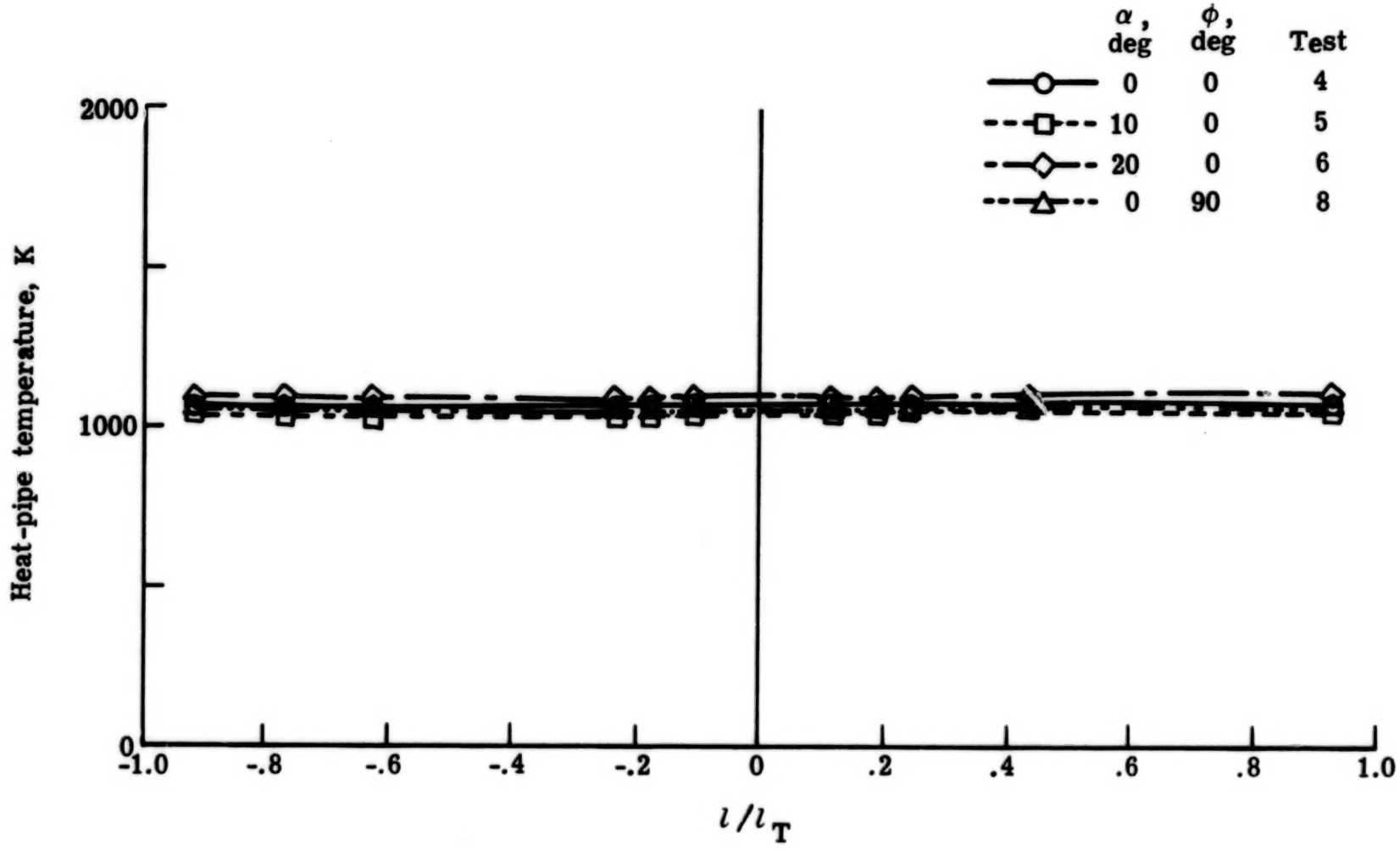

Figure 10.- Chordwise temperature distributions at x/w = -0.02 for various angles of attack and roll.

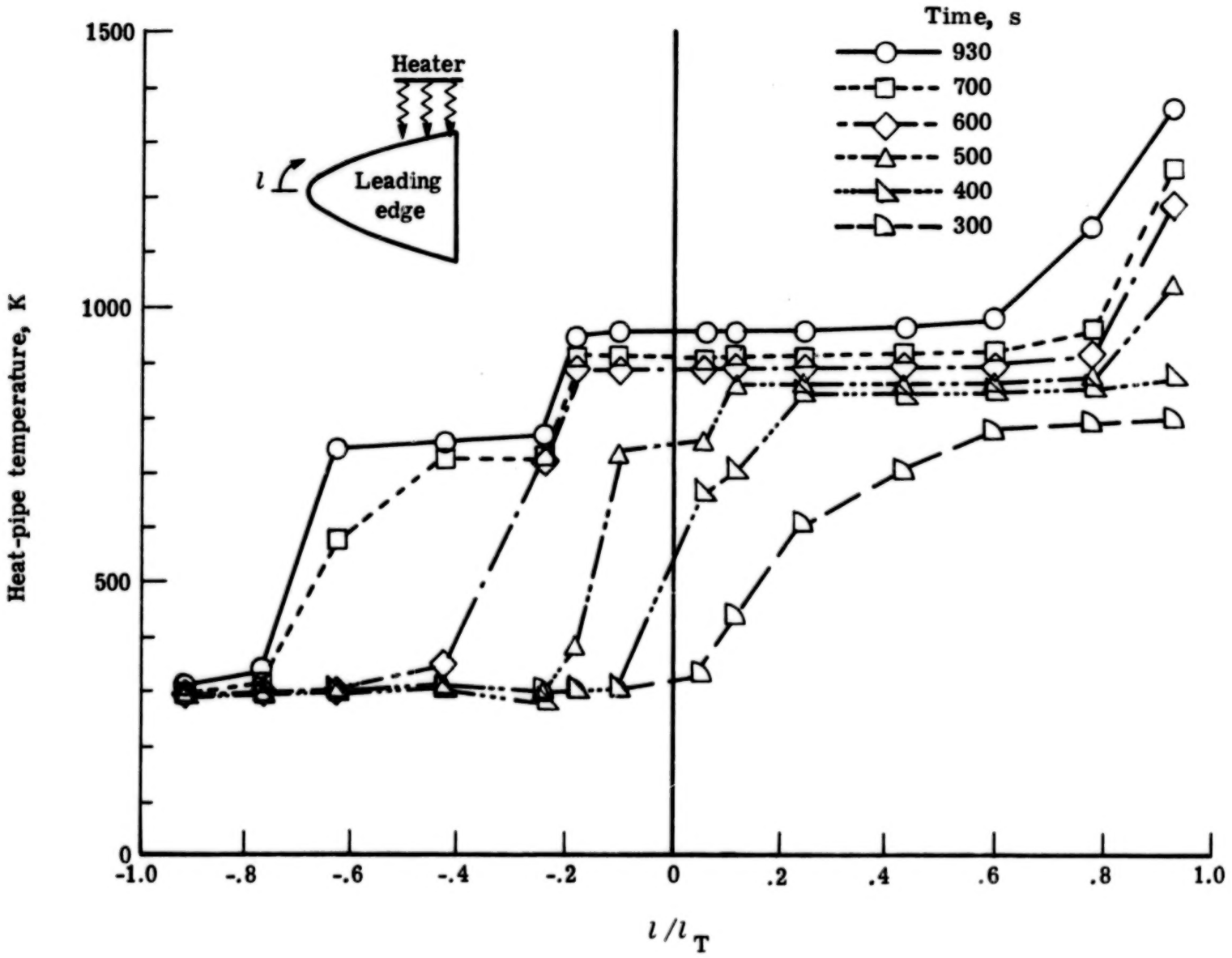

Figure 11.- Temperature distribution caused by exceeding wicking limit.

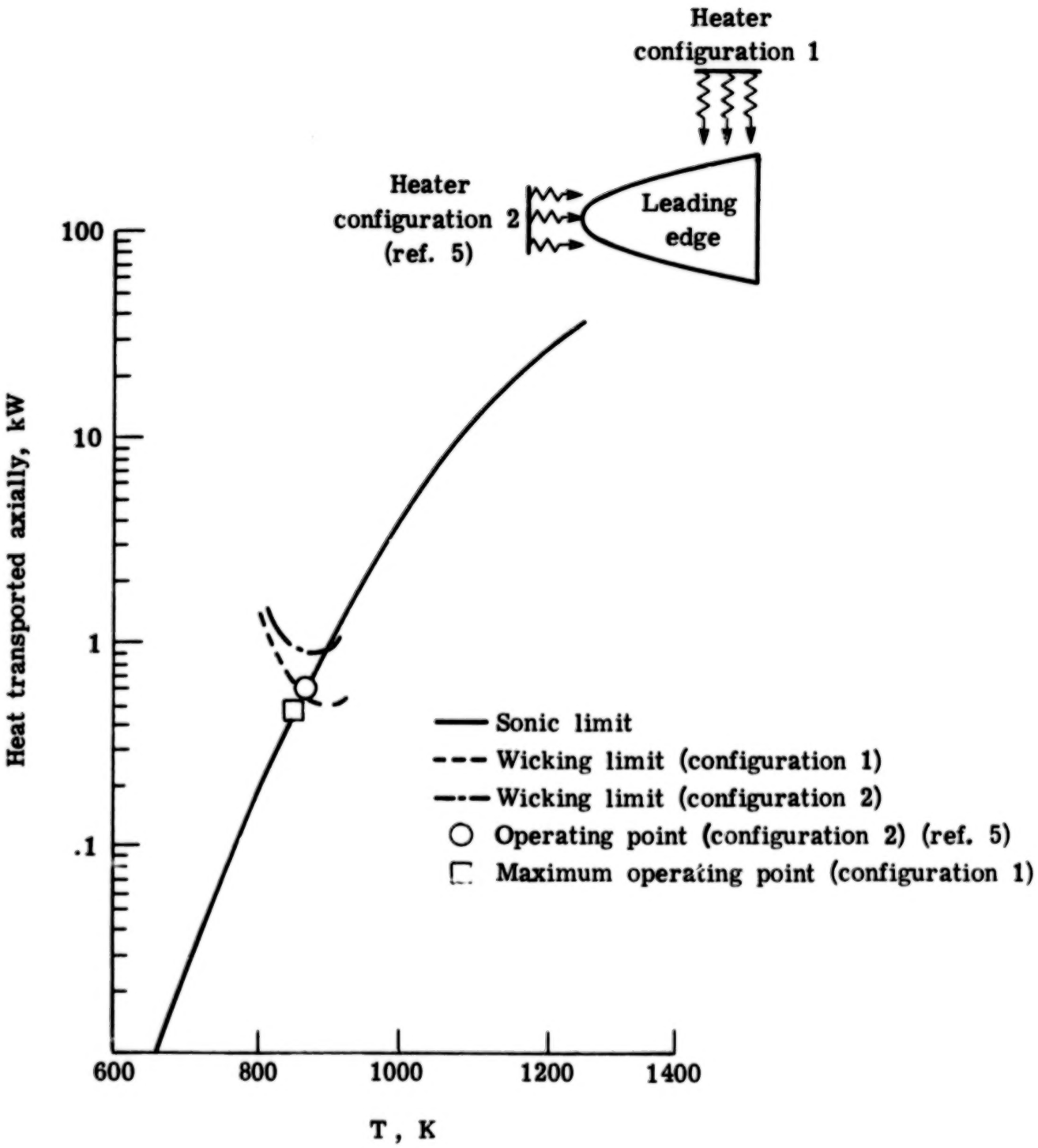

Figure 12.- Heat-transfer performance of heat-pipe-cooled leading edge.

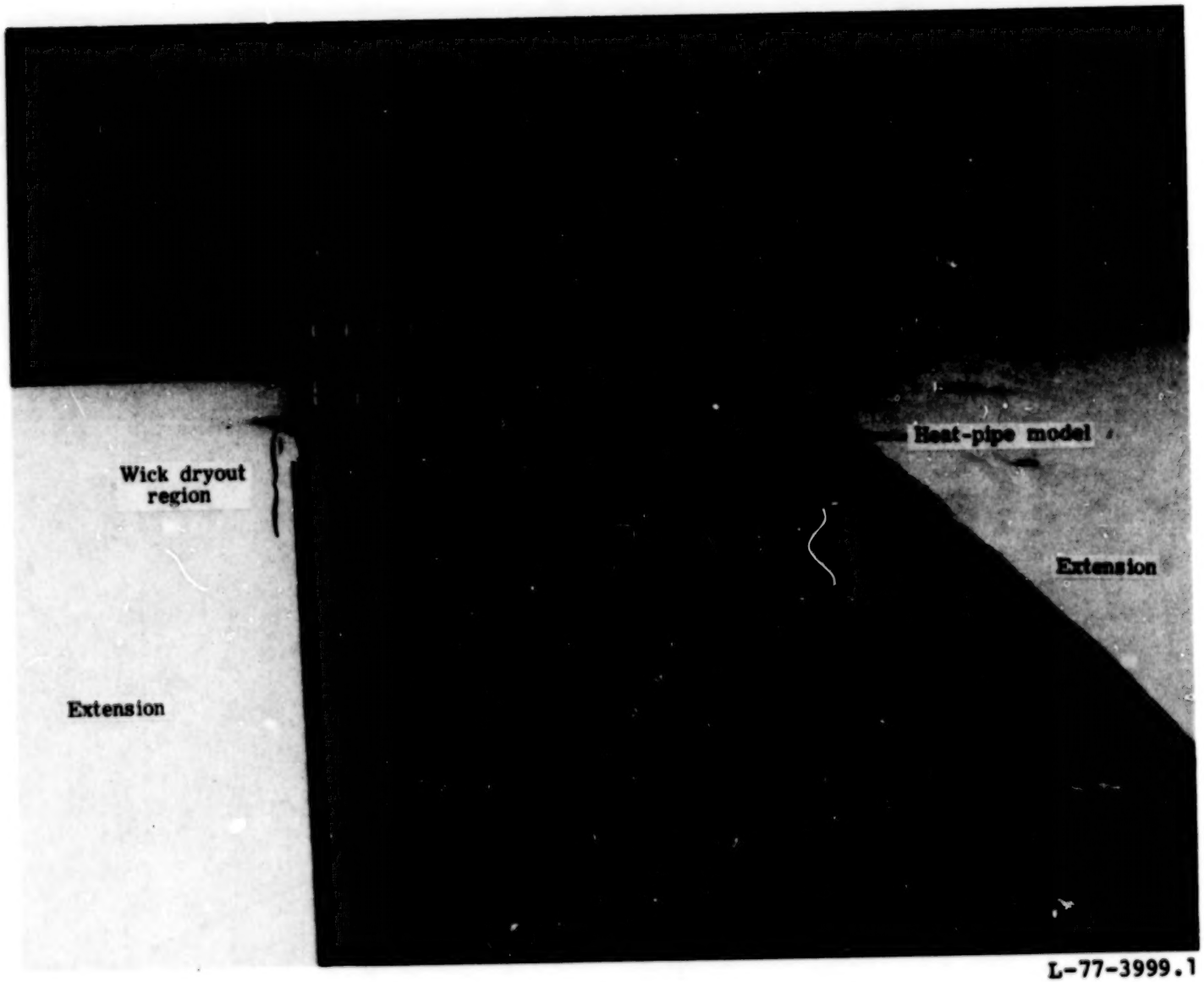

Figure 13.- Thermal buckling caused by lateral constraint of extensions.

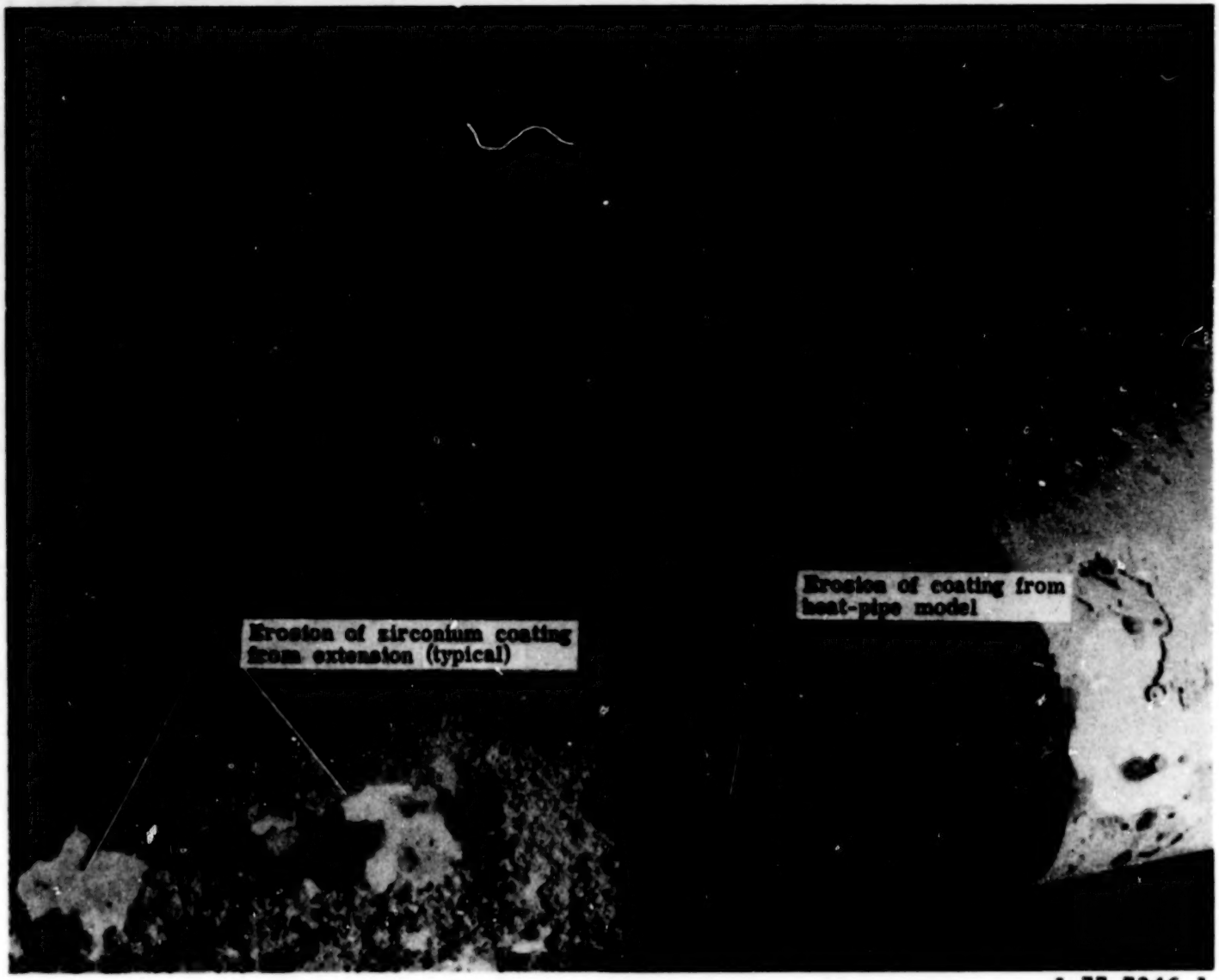

L-77-7346.1

Figure 14.- Extent of erosion damage to heat-pipe model and extensions after test 2.

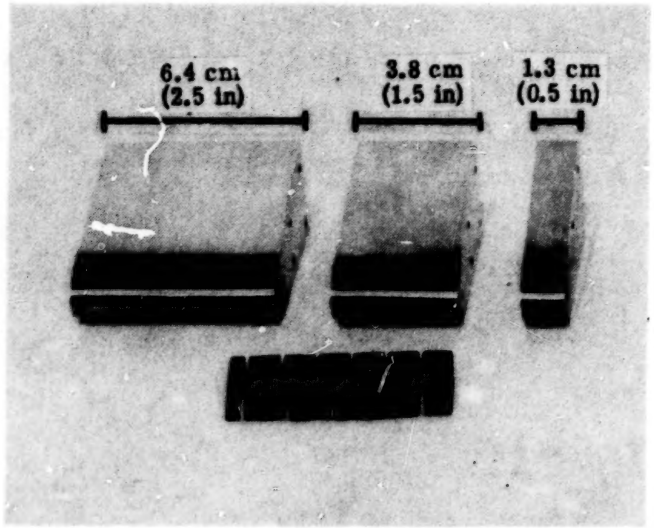

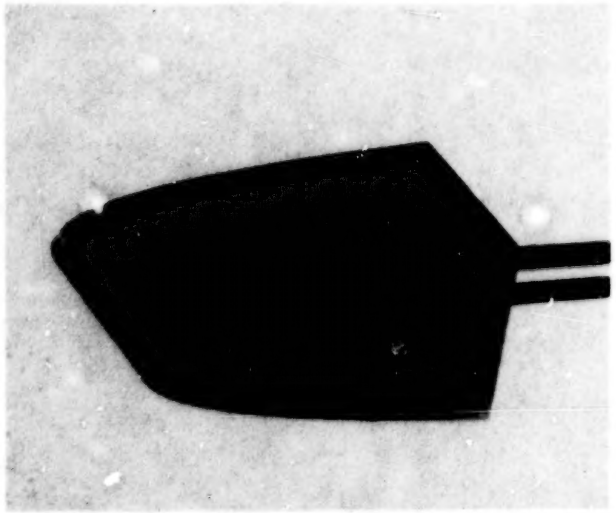

Without aerodynamic fences

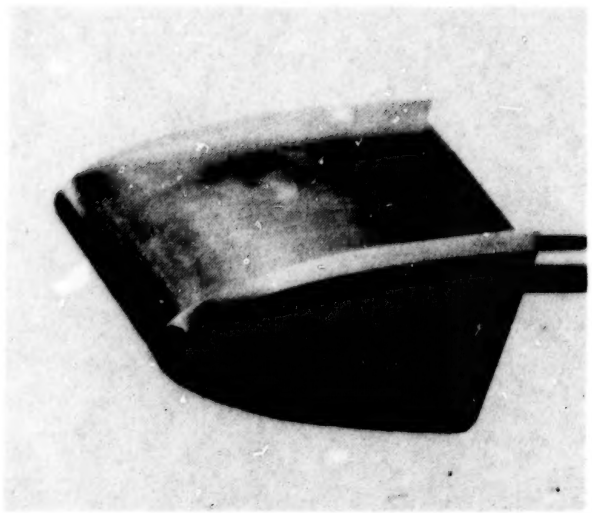

With aerodynamic fences

L-78-139

Figure 15.- Flow study models.

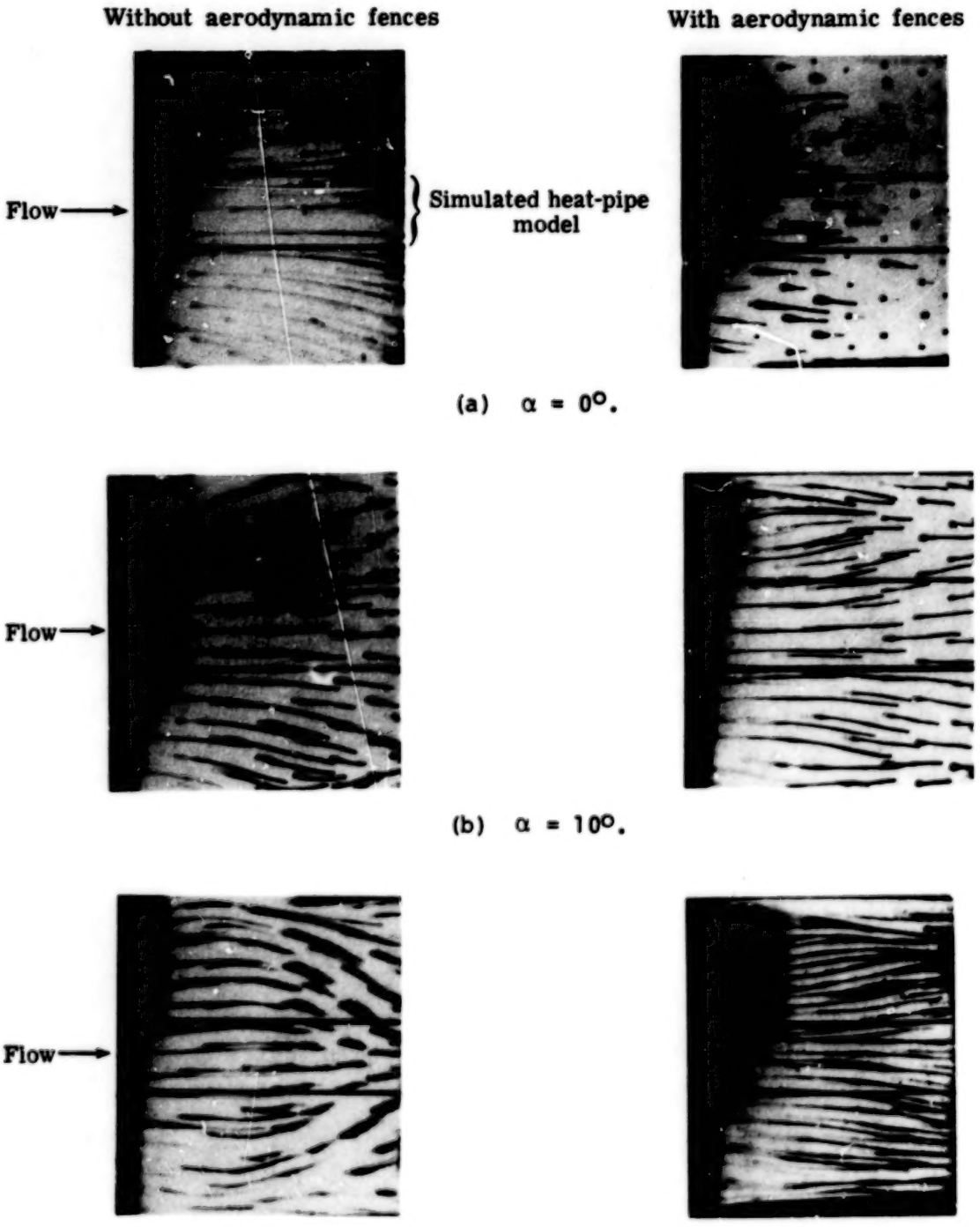

L-78-140

Figure 16.- Oil-flow patterns over leeward surface of 5.72-cm (2.25-in.) span model.

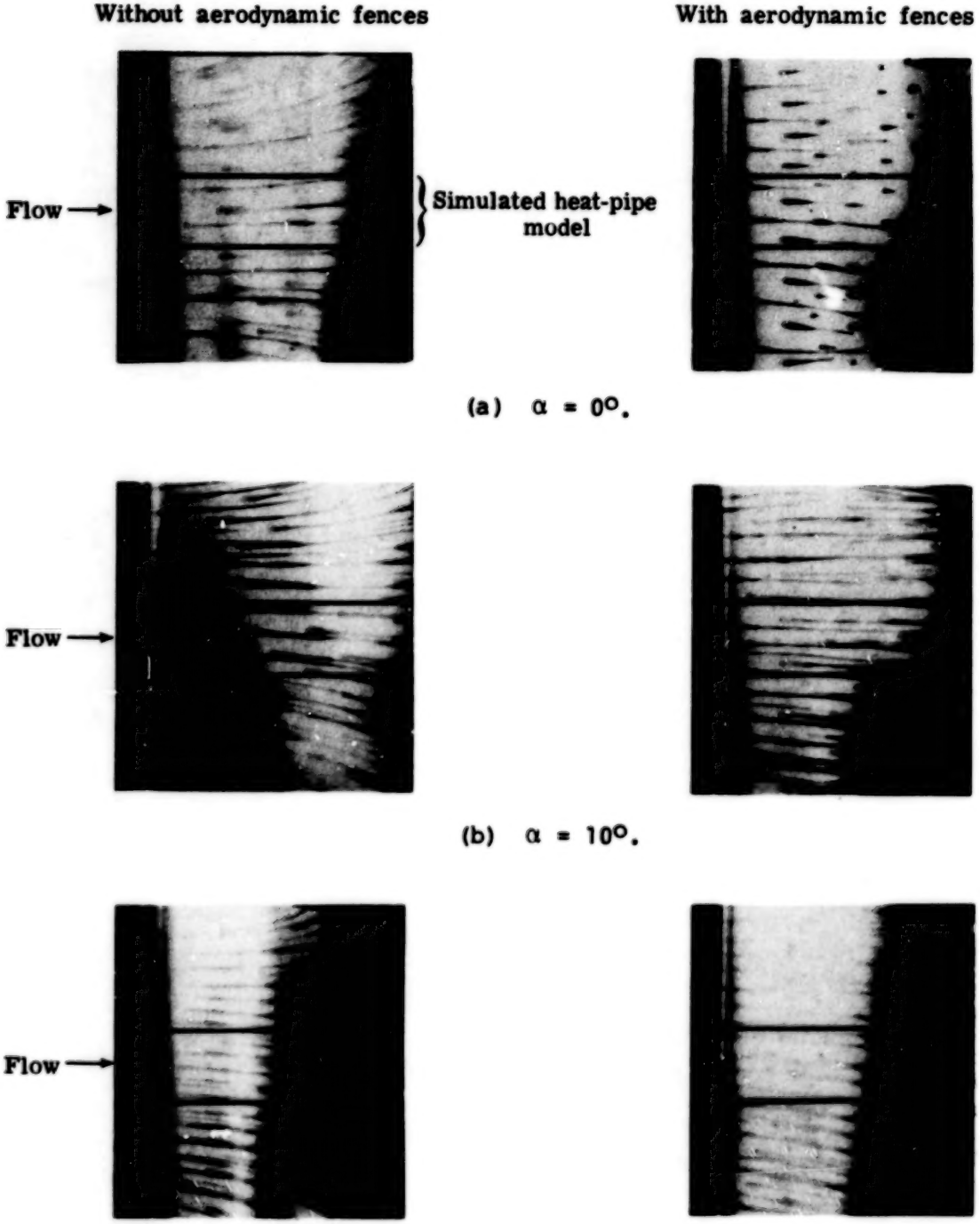

(a) $\alpha = 0^{\circ}$.

(b) $\alpha = 10^{\circ}$.

(c) $\alpha = 20^{\circ}$.

L-78-141

Figure 17.- Oil-flow patterns over windward surface of 5.72-cm (2.25-in.) span model.

1. Report No.	2. Government Accession No.	3. Recipient's Catalog No.
NASA TP-1320		

4. Title and Subtitle	5. Report Date
AEROTHERMAL TESTS OF A HEAT-PIPE-COOLED LEADING EDGE AT MACH 7	November 1978
	6. Performing Organization Code
7. Author(s)	8. Performing Organization Report No.
Charles J. Camarda	L-12302
	10. Work Unit No.
9. Performing Organization Name and Address	506-17-43-01
NASA Langley Research Center Hampton, VA 23665	11. Contract or Grant No.
	13. Type of Report and Period Covered
12. Sponsoring Agency Name and Address	Technical Paper
National Aeronautics and Space Administration Washington, DC 20546	14. Sponsoring Agency Code

15. Supplementary Notes

16. Abstract

A sodium-filled, Hastelloy® X, heat-pipe-cooled leading-edge model, which had previously been tested in a radiant-heating environment, was subjected to steady-state, Earth-entry aerothermal loads (heat and pressure) in the Langley 8-foot high-temperature structures tunnel to verify performance in a realistic hypersonic environment. The model was tested at angles of attack of 0°, 10°, and 20°, angles of roll of 0° and 90°, calculated stagnation heating rates ranging from 244 to 422 kW/m^2 (21.5 to 37.2 Btu/ft^2-s), and nominal stagnation pressures of about 50 and 124 kPa (7.3 and 18 psia). Experimental results were in good agreement with analytical results and indicated that heat pipes could accommodate very intense localized heating and effectively isothermalize structural components. Specifically, results of the tests indicated that the use of heat pipes for leading-edge cooling was a feasible method for lowering localized stagnation temperatures of hypersonic cruise vehicles and space transportation system vehicles sufficiently to allow the use of available and durable superalloys for such applications.

17. Key Words (Suggested by Author(s))	18. Distribution Statement
Temperature control Leading-edge cooling Space shuttle orbiters Aerothermal testing Heat pipes Heat transfer	Unclassified - Unlimited Subject Category 77

19. Security Classif. (of this report)	20. Security Classif. (of this page)	21. No. of Pages	22. Price*
Unclassified	Unclassified	36	$4.50

* For sale by the National Technical Information Service, Springfield, Virginia 22161

NASA-Langley, 1978

37

END

MAR 16 1979